DTMR

TMRSDRS037 Barron River (Kuranda) Bridge (7799) Brittle Fracture Assessment & Management

Investigation of Brittle Fracture Risk and Structure Capacity

267958/Rep002

Draft 2 | 28 January 2021

Job number 267958

Arup Pty Ltd ABN 18 000 966 165

Arup
Level 4, 108 Wickham Street
Fortitude Valley
QLD 4006
GPO Box 685 Brisbane QLD 4001
Australia
www arup com

ARUP

Document verification

Job title		TMRSDRS037 Barron River (Kuranda) Bridge (7799) Brittle Fracture Assessment & Management		**Job number** 267958
Document title		Investigation of Brittle Fracture Risk and Structure Capacity		**File reference**
Document ref		267958/Rep002		
Revision	**Date**	**Filename**	267958-Report02-d1.docx	
Draft 1	14 Oct 2020	**Description**	First draft for client review	
			Prepared by	Checked by	Approved by
		Name	NR	NR	NR
		Signature			
Draft 2	28 Jan 2021	**Filename**	267958-Report02-d2.docx	
		Description		
			Prepared by	Checked by	Approved by
		Name	NR	NR	NR
		Signature			
		Filename		
		Description		
			Prepared by	Checked by	Approved by
		Name			
		Signature			
		Filename		
		Description		
			Prepared by	Checked by	Approved by
		Name			
		Signature			
			Issue Document verification with document		✓

Contents

Tables

Figures

Executive Summary

Recent targeted inspections on the Barron River Bridge by TMR and Arup detected crack like defects in several welds in the bridge main girders. These were confirmed with local removal of the paint and non-destructive testing (NDT) of the bridge steelwork. Barron River Bridge presents a risk of structural failure from cracks in the steelwork due to poor resistance to brittle fracture of the steel plate material.

Currently (December 2020) the bridge is operating with single lane traffic along the bridge centreline to manage the risk and consequences of brittle fracture.

Hazard analysis

Section 2 of the report describes a hazard analysis undertaken determine the plausible risk scenarios for a brittle fracture of the bridge. The following key controls were identified.

- Understand the risk of brittle fracture caused by the applied stresses and material properties of the steelwork through an Engineering Critical Assessment (ECA) .
- Understand the applied stresses at key components and rate of fatigue damage.
- Evaluate the ability of the bridge to redistribute loading in the event of brittle fracture causing a loss of strength in a main bridge girder.
- Evaluate the effects of reduced traffic loads on the bridge and the effects of the vehicle position on the carriageway

Brittle fracture investigation

The investigation has utilised the previous load rating assessment work combined with detailed finite element modelling of the connections to understand the local stresses. The assessment considered the following vehicles across the extents of the deck in two lane, single lane and centreline running configurations.

- 42.5 t 1G semi trailer. DLA 0.4 and 0.1
- 50.5 t Truck and Dog. DLA 0.4 and 0.1
- 79 t Crane. DLA 0.3 and 0.1

The calculated stresses and risk of brittle fracture were then evaluated utilising specialist fracture mechanics software.

The main recommendations from the calculations described are that:

1. The outer running lanes be restricted to 1G and Truck and Dog vehicles only to limit the applied stresses to the edge girder steelwork. Inspections are continued as noted below. In the event of a brittle fracture it is noted that the calculations indicate multiple elements are overstressed.
2. Cranes and other heavy vehicles should not be run in the outer lanes. This is to limit the applied stresses in the edge girders

3. Crane vehicles may be run in the centre lane with additional consideration of stress levels. Inspections are continued as noted below. A 79t crane was assumed for this assessment. A shorter 48 t crane was also checked and found cause similar bending effects to the 79 t crane. Any approvals for this type of loading should be based on the applied stresses rather than the length and weight of the vehicle.
4. A 6-month NDT inspection interval is recommended for the edge girder splice details. Where weld cracks in the splices are removed and a satisfactory reinstatement of the weld undertaken then the inspection interval could be increased to 1 year.
5. A 1-year NDT inspection interval is recommended for the centre girder splice details.

Where the onsite inspections identify a defect then allowable sizes are noted in the tables in section 5.7.1 to 5.7.4.

The durations above are based on expected rate of fatigue crack growth under current traffic. It may be possible to extend the inspection interval if actual stresses are measured via strain gauges to allow for detailed calibration of the calculations. Direct measurement of the stresses in the bridge would allow for an improved load rating of the bridge through use of a measured Dynamic Load Allowance (DLA).

Brittle fracture performance of the bridge

A brittle fracture would only extend through a component of the bridge such as a flange or single girder. The effects of a brittle fracture in a girder is a highly dynamic situation which cannot be accurately calculated. To estimate the likely performance of the overall bridge an investigation of the structure with a fractured girder has been undertaken with the existing grillage model following the recommendations of the TMR Bridge Heavy Load Assessment Criteria (TMR BHLAC). This involved the addition of hinges at the fracture points to represent the local loss of bending capacity. Loads are then transferred to adjacent girders by the cross girders and deck slab.

As noted in section 7 of the report a fracture in the edge girder would be a more significant risk of structural collapse than a fracture in an internal girder. This is demonstrated by the number of elements and magnitude of the SAR values which are less than 1. Additional redundancy could be provided by additional bolting of the cross girders to mobilise the reserve of bending strength which is available in the beam cross section.

The half joint supported spans in span 2 and span 5 can act as structural fuses such that a structural collapse of one span is not expected to cause all spans to collapse.

It is noted that the assessment is carried out for ULS applied loads and ULS capacities however the loading on the bridge at failure would be reasonably expected to be at an SLS level. This application of ULS loads is justified since a brittle failure of a bridge girder would be a highly dynamic structural situation.

1 Introduction

The Barron River Bridge is a composite steel and concrete bridge over the Barron River near Kuranda. It was opened in January 1963 and comprises a six span structure totalling 840' (256m) in length. The main spans are 150' (45.7m) long with 120' (36.6m) end spans. Spans 2 & 5 are suspended spans supported on halving joints with steel rocker bearings to allow thermal movements. The bridge also crosses a non-electrified Queensland Rail track under span 6.

The bridge is currently accessed by 50.5 t Truck and Dog and 42.5 t Semi-trailer vehicles. The original design loading is HS20-16-44 (33 t truck) loading.

Highway bridges in Queensland are traditionally constructed from concrete so the structure is considered a non-standard design. During construction, steel plates for fabricating the girders were only available in limited lengths and combined with difficult site access up the Kuranda Range meant it was necessary join / splice the plates by welding. The splices were constructed both in the fabrication shop and on site as field splices.

Figure 1: Flange lap joint in span 1.

The primary site and shop splices in the main girders utilise a welded lap detail more typical of the termination of a doubler plate on a steel girder. Instead of joining the plates end on with a transverse butt weld, they are joined by tapered overlapping the plates creating a small step. The sides of the overlap are then welded. This detail is very similar to a standard steel girder cover plate detail where a second plate is added to the flange of a girder in areas of high stress.

Whilst the Kuranda Bridge was under construction, the Kings Bridge in Melbourne collapsed in July 1962 due to brittle fracture at a cover plate detail. As a result of the failure, the design of the Kuranda bridge was modified with partial removal of welds at the splice joints and the provision of additional external stressed bars to reduce the stresses in the bridge. This work was completed at the end of 1963 after the bridge was opened to traffic. Refer to Figure 2.

Figure 2: Existing bridge and additional Macalloy strengthening added 8 months after opening.

The bridge carries vehicle loads by behaving as a beam which bends between the supports. This bending causes tension in the bottom flanges of the steel beam and compression on the concrete deck.

The steel within the beam can fail as a result of two main mechanisms.

- **Plastic collapse.** This is a more gradual failure mechanism where the strength of the steel is exceeded by the applied loads (e.g. a very overweight vehicle) and deforms until it fails. This type of failure would be characterised by large deformations (ductility) of the bridge before failure of a member. The failure would be expected to be easily identified by bridge users or inspectors.
- **Brittle fracture.** This is a sudden failure mechanism where a crack can suddenly extend through a steel beam or weld as illustrated in Figure 3. Brittle fracture can occur at low stress levels where a critical combination of sharp flaws (such as cracks), poor material toughness and the repeated loading of many vehicles causes the cracks to grow beyond a threshold for brittle fracture to occur. Unfortunately, these cracks can remain hidden by the paint which is applied to the steelwork for corrosion protection.

Any cracks in the steel can grow as a result of cyclic loading from passing vehicles (fatigue) until a critical crack size is reached that could lead to brittle fracture. The susceptibility of the steel to brittle fracture is partly governed by the fracture toughness property. Fracture toughness varies with the temperature of structural steel.

The steel used in the Kuranda bridge possesses adequate yield strength but has a fracture toughness which is significantly lower than would be specified for a structure of this type to modern design standards. At the typical service temperature there is a risk that small flaws or defects in the structure could pose a risk of brittle failure. Similar welded details in Kings Bridge in Melbourne contributed to brittle fracture in the steel girders and the subsequent repairs and strengthening of the bridge at Kuranda. The Kings Bridge fracture is shown below in Figure 3.

Figure 3: Example of brittle fracture at Kings Bridge Melbourne.

2 Hazard Analysis

A hazard analysis has been undertaken to determine the plausible risk scenarios for a brittle fracture of the bridge. This is based on the 'Bowtie' methodology. Barriers which are identified will then be investigated in the remainder of the report. It is envisaged that the risk scenarios for brittle fracture form part of the overall risks to the structure including bearing movement limits and long term performance of the retrofit PT bars.

The yellow highlighted controls / barriers are discussed within this report to evaluate the risk scenarios. Other controls should be considered by TMR.

Cause	Prevention Controls / Barriers	HAZARD	Reaction Controls / Barriers	Consequences
Visible defect in the steel plates / welds causes brittle fracture to initiate.	Undertake detailed assessment of material properties and impact on performance through Engineering Critical Assessment (ECA)	Loss of load carrying capacity of a bridge girder in Barron River Bridge.	Provide remote traffic control to stop traffic on the bridge.	Loss of life
	Undertake detailed inspection of critical details including removal of paint.		Space vehicles to limit vehicles on parts of the bridge that are structurally independent	
	Monitor temperature of the bridge		Assess collapse mechanism / performance of bridge which has brittle fracture in a girder.	
	Monitor stresses / establish DLA / WIM system		Maintain bridge as three sections so that part of the structure remains serviceable to avoid full replacement.	
	Evaluate transverse distribution of bridge for fractured girder.		Evaluate ability of bridge to redistribute loads to adjacent girders	Structural collapse of part / all of the bridge
	Remove defects and repair. Provide alternative load paths		Limit number of vehicles and position on the bridge / road cross section.	
	Provide improved transverse load distribution between girders to redistribute load around loss of capacity in girder.		Maintain bridge as three sections so that part of the structure remains serviceable to avoid full replacement.	

Cause	Prevention Controls / Barriers	HAZARD	Reaction Controls / Barriers	Consequences
Hidden defect in the steel plates / welds causes brittle fracture to initiate.	Undertake detailed inspection of critical details including removal of paint where no surface defect is visible.		Understand the expected behaviour of the bridge should the beneficial effects of the PT bar be discounted.	*Escalation* Brittle failure may lead to subsequent failure of the PT strengthening bars which are assumed to be able to apply prestress loads across the fracture.
	As per visible defects noted above.		Notify Queensland Rail and stop trains (note only 2 passenger trains per week at Jan 2021)	Train impact into collapsed bridge
Overloading of the bridge due to significantly over mass vehicle	Provide bridge monitoring system for enforcement / weigh in motion (WIM) system. Determine accurate DLA factor for assessment.		Close railway Provide propping or alternative supports for the bridge. Strengthen bridge splices	
	Undertake load rating of bridge to understand behaviour		Maintain bridge as three sections so that part of the structure over the railway remains serviceable should failure occur elsewhere across the bridge.	
	Reduce the loading on the bridge through spaced / single lane running.		Close road	Vehicle collision for vehicles on side road
Failure of the original PT bar strengthening leading to increased stresses in steel flanges	Monitor PT bars		Provide propping or alternative supports for the bridge	
	Install remedial works / replacement / bypass PT bars		Maintain bridge as three sections so that part of the structure remains serviceable to avoid full replacement.	
Poor fracture toughness of original bridge steel plates	Testing of materials to establish material properties		Provide signed alternative routes	Loss of service whilst bridge is repaired.

Cause	Prevention Controls / Barriers	HAZARD	Reaction Controls / Barriers	Consequences
	Monitor bridge steelwork temperature.			
	Undertake detailed assessment of material properties and impact on performance		Establish communication plan	Public concern
Fatigue of bridge steelwork from existing / increasing loading of modern vehicles.	Undertake inspection works in accordance with TMR Inspection requirements.			
	Detailed analysis of the bridge steelwork to understand the rate of fatigue degradation.			
Overstress of bridge steelwork during repair / strengthening of structure.	Undertake detailed analysis of temporary condition of bridge during repairs.			
Errors in assessment leading to unconservative results	Detailed review of calculations and structural modelling			

3 Previous investigation works

The bridge is owned and managed by TMR. The risk of brittle fracture within the bridge was identified by TMR as part of investigations into the long-term durability and performance of the bridge. The investigation works have included replacing, fatigue testing and strength testing, a pair of the stressed bars to determine long term performance of the bars.

Arup were appointed in 2019 to undertake a numerical load rating of the bridge which included investigation of the vertical loading, braking loads and likely movements of the bridge bearings. Fatigue performance of the bridge was also investigated which highlighted that the bridge was towards the end of its fatigue life and may exhibit cracking at multiple locations on the bridge specifically on the bottom flanges of the girders.

It was recommended that a detailed investigation of the brittle fracture risk and a fatigue study be undertaken to understand the residual life of the bridge and allow TMR to develop a proactive management strategy for the structure.

Arup were again appointed in October 2020 to undertake this work with staff from Brisbane and UK based material and structural integrity specialists. Given the specialist work being undertaken, TWI in the UK, a world leading authority in applied fracture mechanics, were appointed to provide independent verification for TMR of the fracture mechanics and fatigue investigations.

An Arup / TMR targeted visual inspection of likely fatigue crack locations was undertaken on 20th + 21st October 2020 as part of the Arup project brief. During this inspection multiple crack like features were identified in the susceptible lap splice details across the bridge, breaking through the painted corrosion protection.

Figure 4: 53mm crack in span 6 edge girder. Note end fillet weld removed during 1962 strengthening

4 Finite element (FE) model

The assessment of the fatigue and fracture sensitive details has been undertaken with detailed partial finite element models of the critical locations. This is shown in the figures below.

4.1 Splice model

The splices at span 1 splice 2 have been identified as the highest risk location due to the potential collapse of multiple spans and applied stress levels.

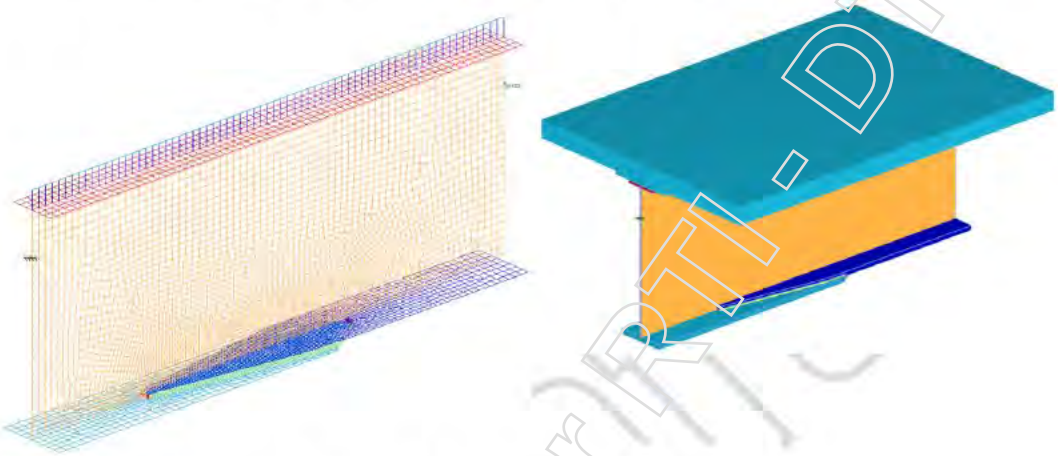

Figure 5: Finite element model of splice Span 1 Splice 2

The stiffness of the deck slab is represented by a single beam element with a rigid connection to the girder since this is remote from the area of interest at the splice.

The weld connecting the overlapping plates is represented by a plane of vertical finite elements which allow the stresses within the welds to be distributed and stress concentration effects to be derived directly. These elements have a thickness representative of the stress area of the weldment, see Section 5.

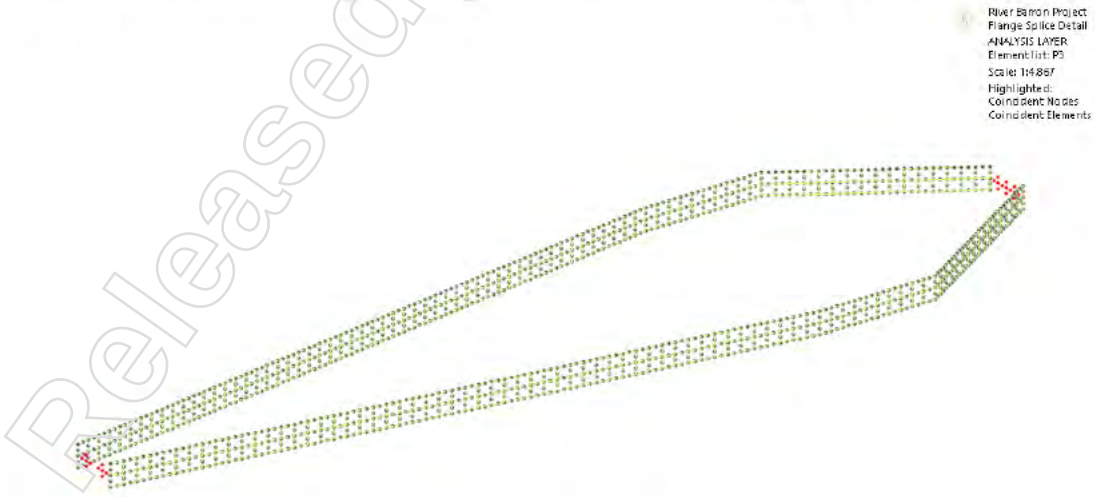

Figure 6: Elements representing the splice welds

Note that the red nodes shown above highlight where the elements representing the end welds have been removed from the model. Where a weld is partially removed by grinding then this can be represented by removing the relevant elements from the analysis model.

To obtain the load effects from the passage of vehicles unit loads of 1000 kNm bending, 1000 kN axial and 100 kN shear are applied to the end of the model.

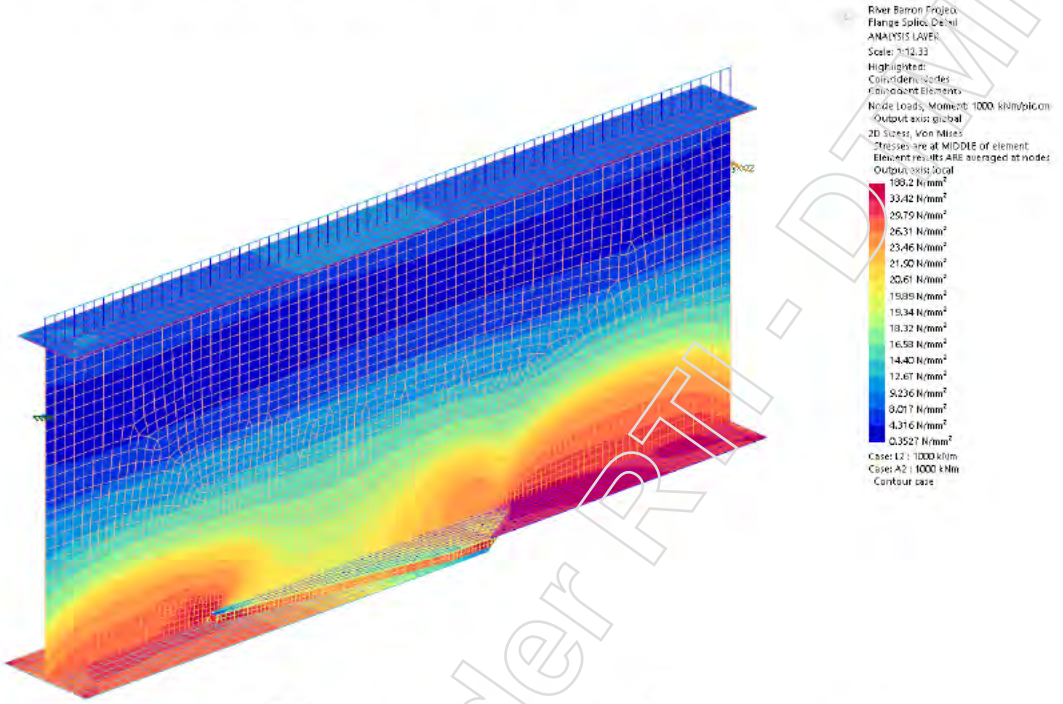

Figure 7: Von Mises Stress in splice detail from 1000 kNm sagging bending moment.

The stresses in the flanges of the FE model are calculated away from the splice detail and compared against a standard section modulus calculation to ensure that the loads applied are distributed to the splice connection as expected. Thus the local effects and stress increases that are determined around the welds can be considered to be representative of the actual bridge.

The load effects from the vehicles are then calculated by factoring the results according to output from the existing grillage model. This is carried out in GSA using the load combinations to combine the bending, axial and shear effects which allows the principal stresses to be directly read from the finite elements which represent the welds and critical toe areas. The model incorporates the effects of live load, dead load and post-tensioning stress.

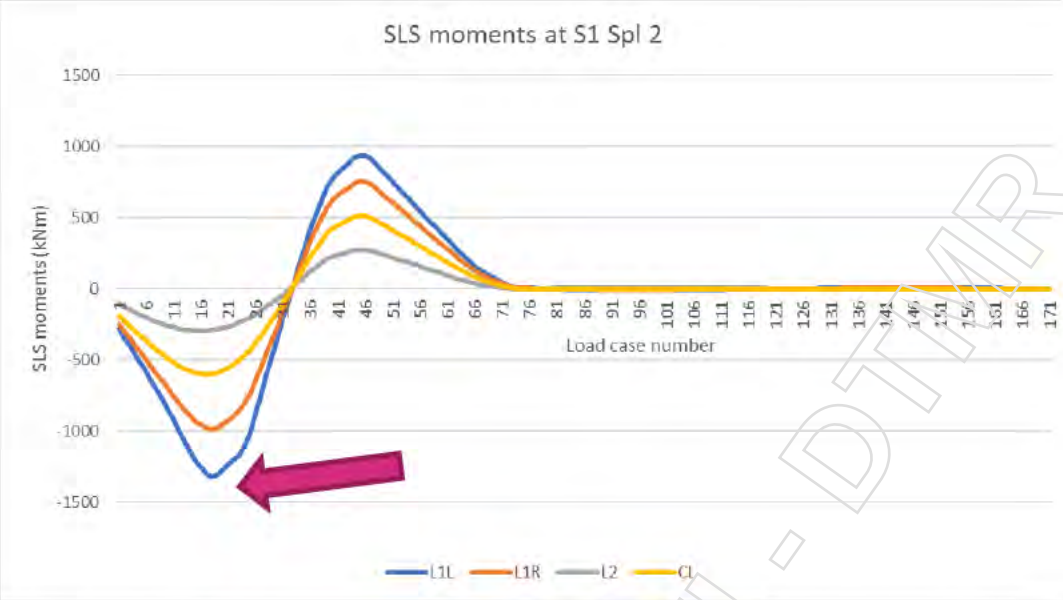

Figure 8: Bending moments in edge girder at splice S1 Spl2 for 1G semitrailer at different lane positions.

For example, for the location shown in Figure 8, the FE results are factored as follows for the vehicle positioned on the edge girder.

*Factored load = -1.328 * bending moment + 0.718 * shear force + 0 * axial force*

These factors are calculated for all positions of vehicle loading at 1m c/c across the bridge. Stresses are then output from the FE model and stress spectra can be derived for weld locations as vehicles pass over the structure. A typical result is shown below in Figure 9 for the end of a weld with the stresses orientated to the span direction.

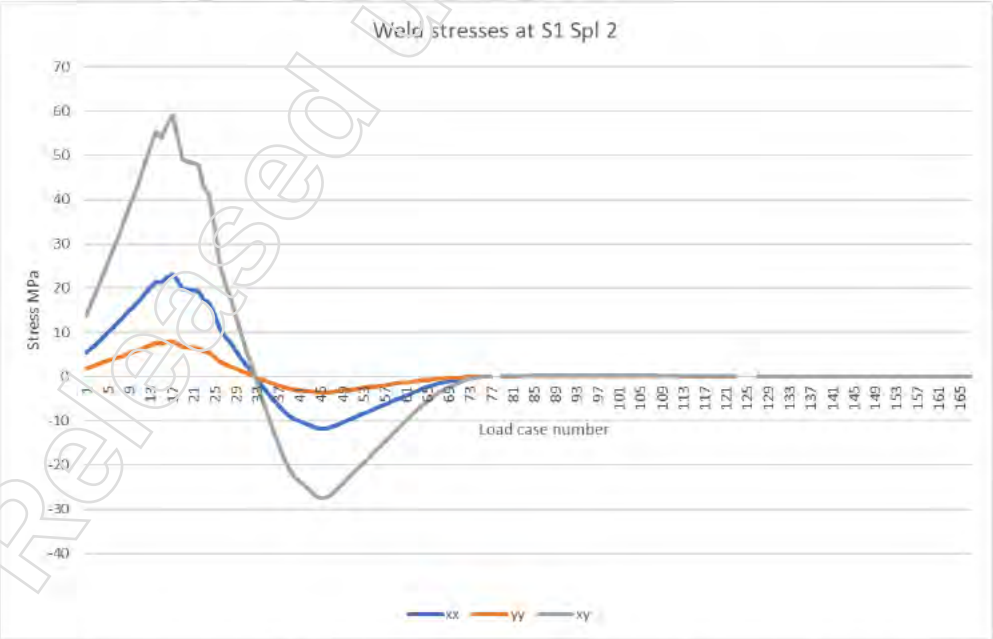

Figure 9: Direct and shear stress spectrum (MPa) at end of weld plotted against vehicle position along bridge (m).

It is noted that the shear stress is significant which is as expected for the fillet weld splice detail.

- xx stresses are parallel to the weld
- yy stresses are vertically perpendicular due to the vertical orientation of the finite elements for the weld.
- xy stresses are the shear stresses on the perimeter of the finite element.

Note that principal stresses and Von-Mises stresses can also be output if required for the ECA and fracture mechanics calculations.

4.2 Cross girder and stiffener model

Stresses at the cross girder stiffener have been investigated with an additional finite element mode as shown below.

Loads are calculated using then same methodology as discussed above.

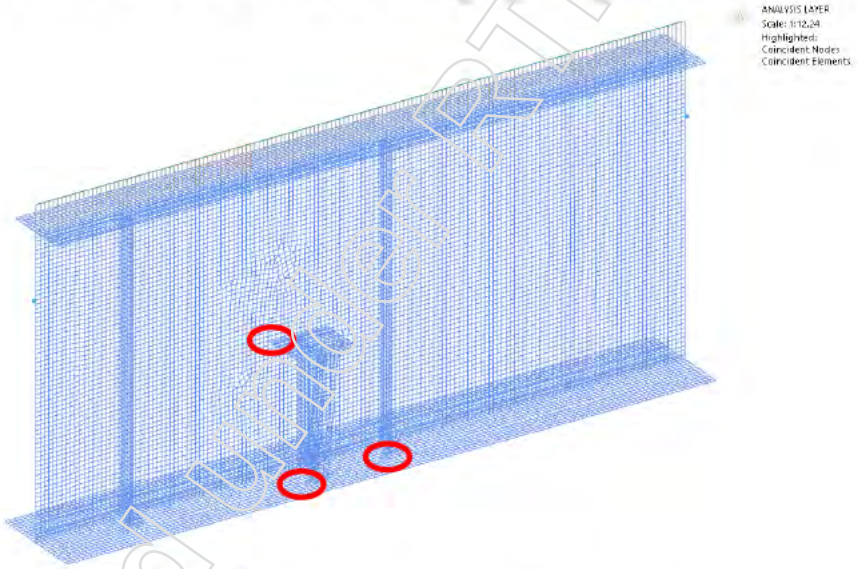

Figure 10: Cross girder and stiffener model with critical sections highlighted.

5 Brittle Fracture – Engineering Critical Assessment (ECA)

Fracture mechanics assessments of defects in the girder flanges have been conducted in accordance to BS 7910:2019. Previously reported, preliminary Engineering Critical Assessment (ECA) identified some large cracks in the splice fillet welds as posing a risk of brittle fracture and these priority 1 cracks have been removed though grinding of the splice welds. ECAs are presented in the following sections for splice welds at the toe and root position in the unground and ground (100mm weld removed) scenarios. Results are presented for edge and centre girders with loading from 42.5 t 1G Semitrailer, 50.5 t Truck and Dog (T+D) and 79t Crane vehicles.

In this section of the report, existing and potential flaws in the structure are assessed to determine the risk of brittle fracture and the critical dimensions under various locations and loading conditions presented.

These results are presented in terms of Option 1 Failure Assessment Diagrams (FADs) which diagrammatically show the proximity of a flaw to a critical limit capturing the risk of brittle fracture and plastic collapse, and critical flaw depth versus length plots which show sensitivity of the measured dimensions of flaws to the risk of fracture. These results are described in Section 5.7, the effects of fatigue crack growth are considered in Section 6, and guidance on managing the effects of brittle fracture risk, fatigue crack growth through NDT inspections is given in Section 8.

5.1 Parameters for Brittle Fracture Assessment

The derivation of parameters relevant to the brittle fracture ECA are given in this section, including any assumptions made.

5.1.1 Fracture Toughness

Fracture toughness is the property of the steel and the geometry around the flaw which resists crack propagation. In the context of the Barron River Bridge, Charpy impact testing has been conducted on samples from the flange and web plates, but not weldments or steel affected by welding processes. Charpy tests are not a quantitative measure of fracture toughness but methods exist to make predictions of fracture toughness which are applied in the following sections.

5.1.1.1 Treatment of Charpy test data

At this stage, the fracture toughness at the critical details must be determined from Charpy impact tests conducted on samples of bridge steel. Test data is available from investigations in 1962 after the failure of the King's bridge, and more recent tests by Bureau Veritas in 2019. The 2019 testing was conducted to AS1544.2.

Testing was conducted on plates 38mm, 32mm, 25mm, and 12mm thick.

The focus on this report is on the 32mm (1.25in) and 38mm (1.5in) plate used in the bottom flange splices where most critical details and visually identified flaws

have been located. 12mm (0.5in) web plate is also considered for defects on the cross girder web connections.

Considerable scatter is observed in the flange plate Charpy test results, the 2019 testing uses 2 coupons per test temperature and the 1962 testing reports only a single result per test temperature.

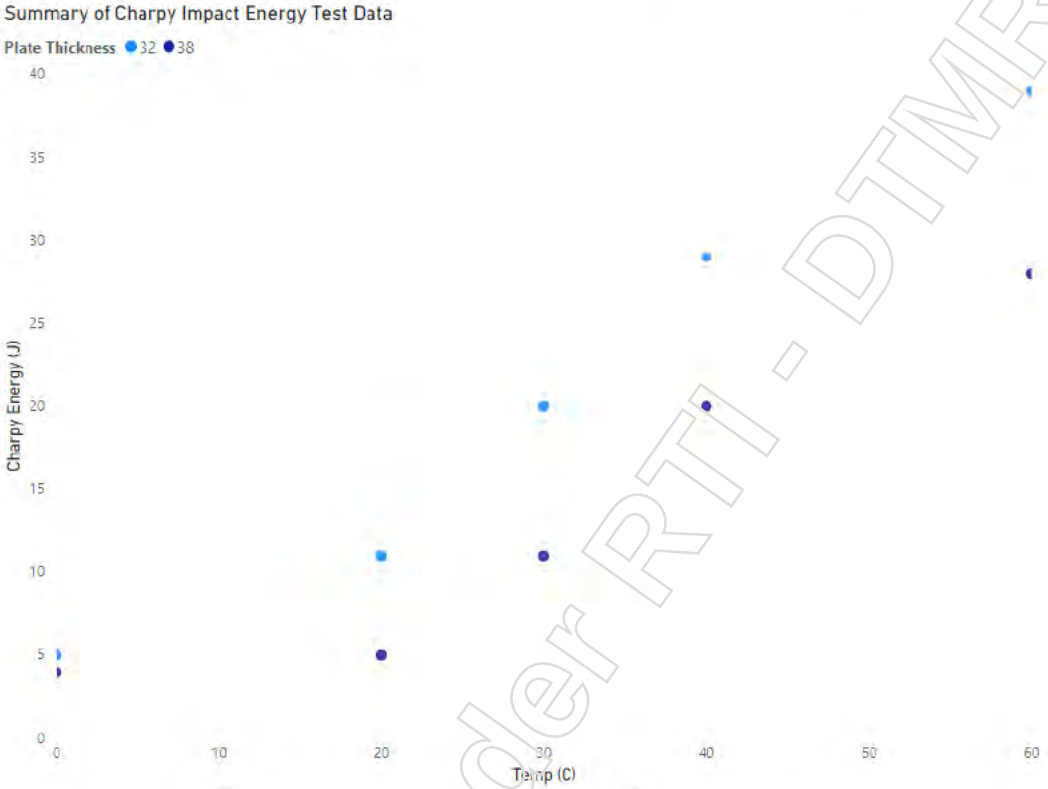

Figure 11: 1962 Charpy testing of flange plate (32mm and 38mm).

Figure 11 shows the 1962 testing for 32mm and 28mm plate used in the flange splice connections. Charpy tests were conducted at a range of temperatures to characterise the transition behaviour of the steel toughness. Single tests only are available at each test temperature, however the data suggests that the lower shelf toughness of both plates is similarly low (4-5J) and that the 38mm plate transitions to ductile behaviour at a higher temperature, i.e. the thicker 38mm plate remains brittle at higher temperatures than the thinner 32mm plate.

Due to the reduced transition temperature of the 38mm plate which has similar, lower shelf, toughness at 20 degrees as 0 degrees, no improvement in toughness has been considered for ECAs at ambient (~20 degrees).

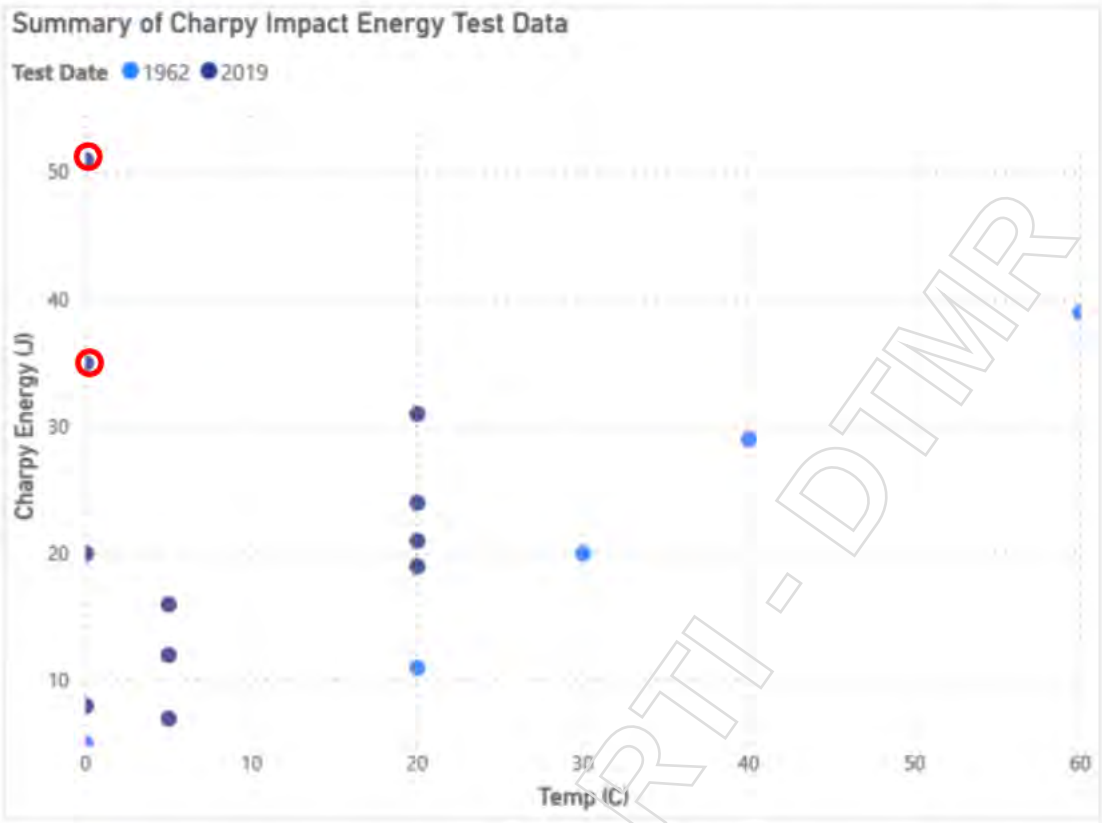

Figure 12: 32mm plate, Charpy impact energies. 1962 and 2019 test data*

*Note two, outlying, high value Charpy tests at 0 degrees have not been included in the estimates for fracture toughness.

Figure 12 shows the additional 2019 test data for the 32mm plate (38mm plate was not tested in 2019), the testing shows increased scatter and that the 1962 testing is consistently reporting lower toughness.

ISO 148-1:2016, which covers the test method for Charpy pendulum impact testing, covers measurement uncertainty in informative Annex E. Although insufficient information is available from the test data to fully characterise the uncertainty in the measured values, some simple statistical assessment can be made on the dataset.

For the purposes of this study, all 32mm Charpy tests are combined into a single dataset include retests. The uncertainty of the mean value of n test specimens is defined as:

$$u(\bar{x}) = \frac{s_x}{\sqrt{n}}$$

Where, $u(\bar{x})$ is the uncertainty of the mean value, $\bar{x}$ is the mean value, s_x is the standard deviation of the test samples, and n is the number of test specimens.

Temp (deg c)	Mean, $\bar{x}$ CVN (J)	Max CVN (J)	Min CVN (J)	Range CVN (J)	s_x	$u(\bar{x})$ ISO 148 (J)	Reliable Min CVN ($\bar{x}$ - $u(\bar{x})$) (J)
0	11.4	20.0	4.0	16.0	7.1	3.2	8.2
5	11.7	16.0	7.0	9.0	3.7	2.1	9.5
20	18.5	31.0	5.0	26.0	8.5	3.5	15.0
30	15.5	20.0	11.0	9.0	4.5	3.2	12.3
40	35.0	29.0	20.0	9.0	4.5	3.2	31.8
60	33.5	39.0	28.0	11.0	5.5	3.9	29.6

Table 1 Summary of Charpy impact test results for 32mm and 38mm flange plate

From Figure 12 considerable scatter on the Charpy test data is evident, include measured energies at 0 degrees exceeding all other test values. No clear brittle to ductile transition is clear from the combined test data, however it can be stated that typically the steel is behaving in a brittle manner with the majority of tests under 27J at typical ambient temperatures; The trend is for lower toughness at lower temperature, as would be expected for ferritic steels.

The simple statistical analysis summarised in Table 1 for the test temperatures with multiple measurements, show high standard deviations, and high mean uncertainty. Reliable minimum impact energies determined using Annex E of ISO 148-1 have been calculated.

Section 7.1.4 of BS7910:2019, discuss statistical treatment of fracture toughness test data. Whilst Charpy Impact testing is not a quantitative measure of fracture toughness some of the principles of treating test data are considered here. The Minimum of Three Equivalent (MOTE) approach could be considered on this data set, particularly on the 0 degrees C tests, however this would yield similar estimates of lower bound Charpy impact energy to the prior approach discussed. It is also not possible to confirm similarity in fractures from inspection of the coupon fracture faces.

It is expected that fracture samples in the brittle and transition region will exhibit more scatter than those in the ductile region. Given the uncertainty, and limited number of samples, in the test data the following estimates are considered for the Charpy impact energy:

	Lower Bound	Upper Bound
Min Service Temperature (deg C)	Min Charpy impact energy (J)	Reliable Min Charpy impact energy (J)
20	5*	15
5	7	9.5
0	4*	8.2

Table 2 Flange plate Charpy impact energies considered for sensitivity studies

*Note minimum impact energy from 1962 testing of 38mm flange plate

A similar process was taken for the web plate, the following estimates were considered for the Charpy impact energy:

	Lower Bound	Upper Bound
Min Service Temperature (deg C)	Min Charpy impact energy (J)	Reliable Min Charpy impact energy (J)
20	41.0	46.5
5	24.0	34.1
0	24.0	28.3

Table 3 Charpy impact energies considered for sensitivity studies, 12mm plate

5.1.1.2 Fracture Toughness Estimate

The discussion in Section 5.1.1 concludes that considerable scatter is present in the Charpy impact test results for the flange plate. No prediction of brittle to ductile transition can be made from the test data. It is also not possible to identify the T_{27J} temperature from this test data.

Therefore, according to equation J.1 Annex J BS7910:2019, K_{at} is estimated at single temperatures. Equation J1 applies to near lower shelf behaviour where <27J Charpy impact energies are recorded at single temperatures, as is the case for the flange plate test data. The recorded Charpy results for the flange plates are typically below 27J at all tested temperatures.

$$K_{mat} = \left[\left(12\sqrt{C_v} - 20\right)\left(\frac{25}{B}\right)^{.25}\right] + 20$$

Where C_v is the Charpy impact energy and B is the plate thickness.

The estimated fracture toughness for the lower and upper bound Charpy energies shown in Table 2 are provided in Table 4 below.

Min Service Temperature (deg C)	Min Charpy impact energy (J)	K_{mat} (MPa$\sqrt{m}$)	Reliable Min Charpy impact energy (J)	K_{mat} (MPa$\sqrt{m}$)
20	5*	37.8	15	47.8
5	7	30.6	9.5	36.2
0	4*	23.6	8.2	32.5

Table 4 Kmat estimates of fracture toughness for flange plate.

For the web plate, at 0 degrees the reliable minimum Charpy energy from the test data shown in Table 3 is 28.3J. For a fracture toughness estimate, it has been assumed that 0 degrees represents T_{27J}, the temperature at which 27J impact energy is absorbed. Using Equation J.4 Annex J BS7910:2019, a fracture toughness estimate for the web plate at 0 degrees is 64.2 MPa$\sqrt{}$m.

Note that Charpy impact tests were only conducted on steel samples taken from unwelded parts of the bridge girders. No testing has been conducted on weld metal or HAZ microstructures. Welding can cause brittle microstructures to develop leading to reduced fracture toughness compared to the parent metal.

Although no estimate of this reduction can be made, the statistical treatments discussed above and the lower bound estimates of K_{mat} are likely to be sufficient to account for reduced weld toughness.

Note that in the bottom flange splices different steel gauges are present (31.75mm and 38.1mm). The thickness of the plate influences fracture toughness due to constraint effects and for the plate fracture toughness estimates, the lower bound thickness has been considered. The difference is minimal (1-2%).

The recommended fracture toughness to be used for ECA are shown in Table 5 below.

ECA Location	K_{mat} (MPa√m) – 0 degrees
Flange	32.5
Web	64.2

Table 5: K_{mat} estimates used for ECA.

5.1.2 Steel Mechanical Properties

The mechanical properties of the steel determine the load ratio (proximity to plastic collapse) and the bounding line of the Failure Assessment Diagram (FAD). The yield strength of the material also governs the upper bound magnitude of tensile residual stress due to welding, see Section 5.5. Values for the parent metal are available from the same test samples as described in Section 5.1.1.

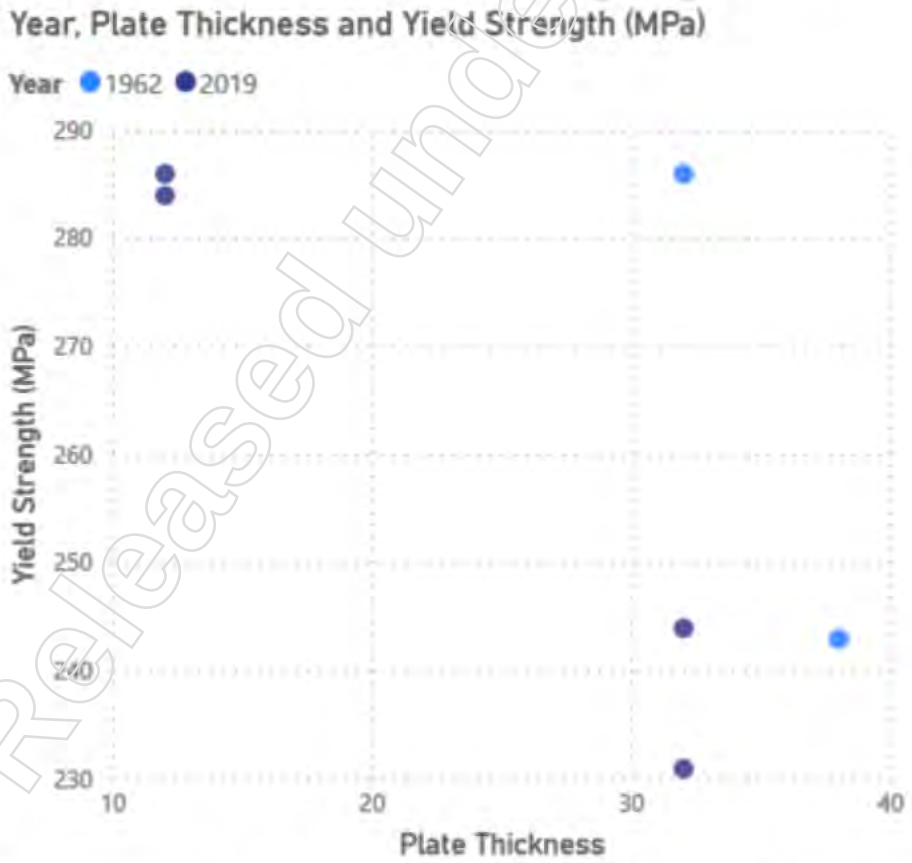

Figure 13: Yield strength test results (tensile) for all plate samples, flange and web.

For the flange plates the 2019 testing provides the lower bound yield strength of 231 MPa and tensile strength of 446 MPa. The 32mm and 38mm flange plate show similar mechanical properties and these values capture the lower bound of the two flange plate thicknesses.

For the web plates 2019 test date only is available which provides a lower bound yield strength of 284 MPa, the lower bound tensile strength is 488 MPa.

The yield strength and tensile strengths are used along with an assumed elastic modulus of 205 GPa and a Poissons ratio of 0.3, considered typical for structural steel at the expected service temperatures.

Note that no test data or samples are available for the mechanical properties of the weld metal. General weldments exhibit higher yield strengths than the parent metal, in this assessment the parent metal mechanical properties have been assumed for flaws characterised in the HAZ and weld metal.

5.2 Flaw Characterisation

Inspection of the structure has identified numerous flaws. A range of flaw characterisations have been considered for ECAs to cover the range of flaws identified and other potential at risk locations, such as plate defects in the low toughness bottom flanges.

Flaws were previously identified in the bridge and classified as priority 1, 2 and 3. Priority 1 cracks located in the bottom flange splice welds, have been removed or ground leaving small residual root defects. In Sections 5.2.1, and 5.2.2 the approach for characterising the types of flaws seen in the structure are discussed, and general considerations are described below.

Flaws are idealised as sharp tipped semi-elliptical flaws, as shown in Figure 14. For critical flaw size calculations, a range of flaw aspect ratios are considered from a/2c=0.025 to a/2c=0.4. This range of aspect ratios covers the range of flaws detected through NDT, where long defects have been identified.

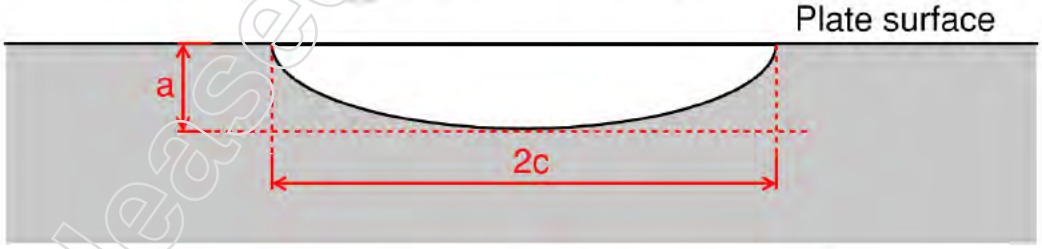

Figure 14: Surface flaw idealisation and dimensions: Depth a, length 2c.

The flaws considered have been split into three sections discussed below.

5.2.1 Flaws in Bottom Flange Splice Welds

From investigations on the structure, the predominant type of flaw present in the splice welds is likely to be a crack initiated from the root of the splice plate at the end of the splice plate, where the original weld was removed in the 1960s. The

crack has propagated through the weld, with the crack front exposed in the weld throat. Where priority 1 defects have been removed by grinding the cracked weld, it has been observed that the flaw extends further along the weld at the root than the exposed surface, leaving a residual root defect.

Based on these observations, and general considerations about the structure, a series of flaws have been postulated which allow a management strategy to be developed such that critical flaws in the structure can be identified and remedial actions taken until the risk of brittle fracture is reduced.

The flaws that are considered for the ECA are as follows:

1) Flaws at toe of weld between bottom flange splices (unground, as fabricated condition).
2) Flaws at root of weld between bottom flange splices.
   a) At the start of the weld (tapered section), through thickness defects are considered to identify the critical length (priority 1 flaws)
   b) For ground welds where up to 100mm of weld is removed, the critical dimension of the residual root defect is identified.

The typical splice weld defect assessed is shown diagrammatically in Figure 15 below.

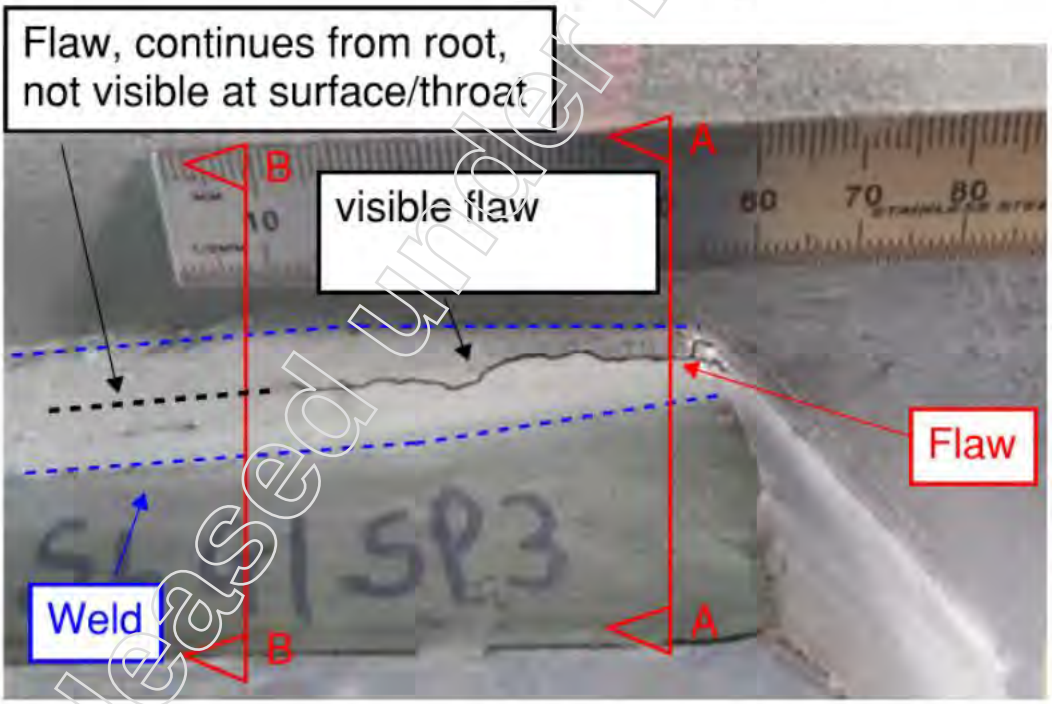

Figure 15: Typical weld defect identified and diagram showing flaw assessed in ECA.

Cracks observed in the splice welds have initiated in the weld root and propagated at approximately 45 degrees towards the surface of the weld. The crack front through the weld is therefore typically seeing a range of stress components which can include shear. As a result, a conservative approach is to take the maximum principal stress acting through the connection for the ECA.

5.2.1.1 Type 1 Flaw Characterisation

The type 1 flaw characterisation is a postulated flaw at the toe of the bottom flange splice welds. Defects have not been identified at these locations; however, the weld toe is a typical location for weld defects and fatigue cracks. ECAs have been prepared for this onerous condition to enable classification of any defects identified in this location.

The characterisation of the flaw is shown in Figure 16. The flaw is assessed as a surface defect in flat plate. The plate thickness is taken as the full flange thickness and a Mk factor is assumed to account for the weld toe profile. A range of aspect ratios have been considered: a/2c=0.025, a/2c=0.1,a/2c=0.4.

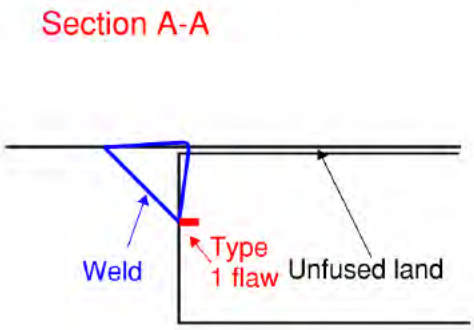

Figure 16: Type 1 flaw characterisation shown on Section A-A from Figure 15.

5.2.1.2 Type 2a Flaw Characterisation

The type 2a flaw characterisation represents a typical flaw identified in the structure. It considered the through thickness root defects that have been visually identified through inspection.

The characterisation of the flaw is shown in Figure 17. The flaw is assessed as a through thickness defect in flat plate. The plate thickness is taken as the weld effective throat, including the tapering/blending of the weld undertaken in the 1960s.

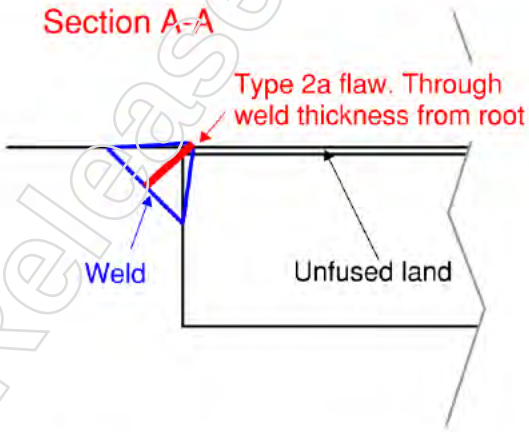

Figure 17: Type 2a flaw characterisation shown on Section A-A from Figure 15

5.2.1.3 Type 2b Flaw Characterisation

The type 2b flaw characterisation represents the residual root flaw identified in the structure after priority 1 cracks have been ground out. It considered the residual root defect that can be identified in the exposed weld termination after grinding.

The characterisation of the flaw is shown in Figure 18. The flaw is assessed as a surface defect in flat plate. The plate thickness is taken as the weld effective throat. An Mk factor is included to consider stress magnification due to the profile of the root area. It is difficult to identify the length of this flaw type with NDT due to the proximity of the unfused land, therefore a range of aspects ratio are considered to determine safe flaw heights. Aspect ratios considered are a/2c=0.005, 0.025 and 0.1, these small aspect ratios account for potentially very long residual defects that continue to run along the weld root.

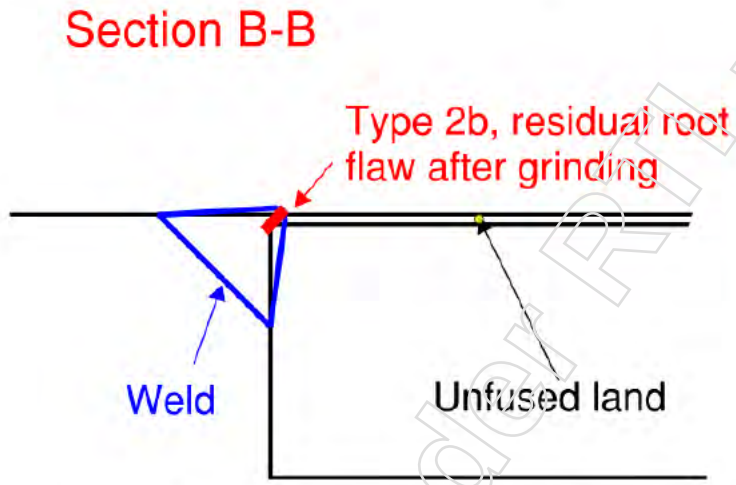

Figure 18: Type 2b flaw characterisation shown on Section B-B from Figure 15

5.2.2 Flaws at Cross Girder Web attachments

Flaws have been identified at or near the toes of fillet welded attachments to the girder webs. An example is shown in Figure 19 from Cross Girder 3.

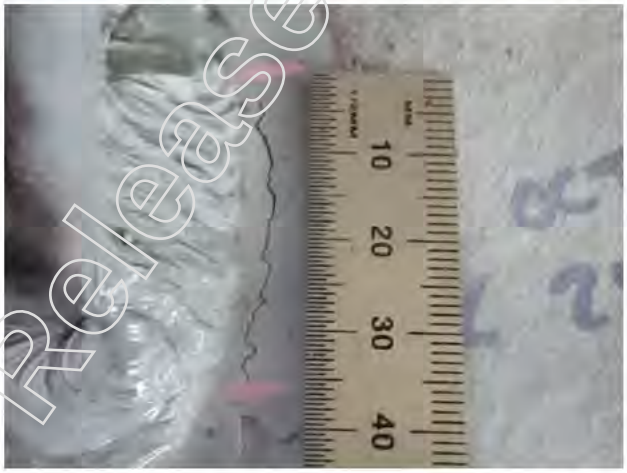

Figure 19: Crack at weld toe/HAZ, Cross Girder 3 flange to Web G1.

Critical flaw dimensions have been determined for defects at the weld toe of attachments to the girder webs. Note that additional material information is available for the web plates which is summarised in Section 5.1.

A range of aspect ratios are considered as stated in Section 5.2. The flaw shown in Figure 19 has measured length (2c) 35mm by MPI and measured depth (a) 3.3mm by ACFM, giving an aspect ratio a/2c of 0.09.

5.3 Detailed Finite Element Models

Detailed Finite Element models have been prepared for the bottom flange splice connections and web stiffener attachments. The methodology for loading the detailed finite element models and calibrating the load factors to the global grillage model is detailed in Section 4. This section of the report explains how appropriate stresses for the ECA have been extracted from the detailed models.

5.3.1 Bottom Flange Splice Connection

A detailed finite element model of the splice connection has been developed to determine the magnitude and direction of stresses in the splice connections, accounting for geometrical stress concentrations from the splice geometry. The weld profile is not modelled explicitly, and these effects are accounted with the Mk factor discussed later in this section.

The detailed splice model is shown in Figure 20 below.

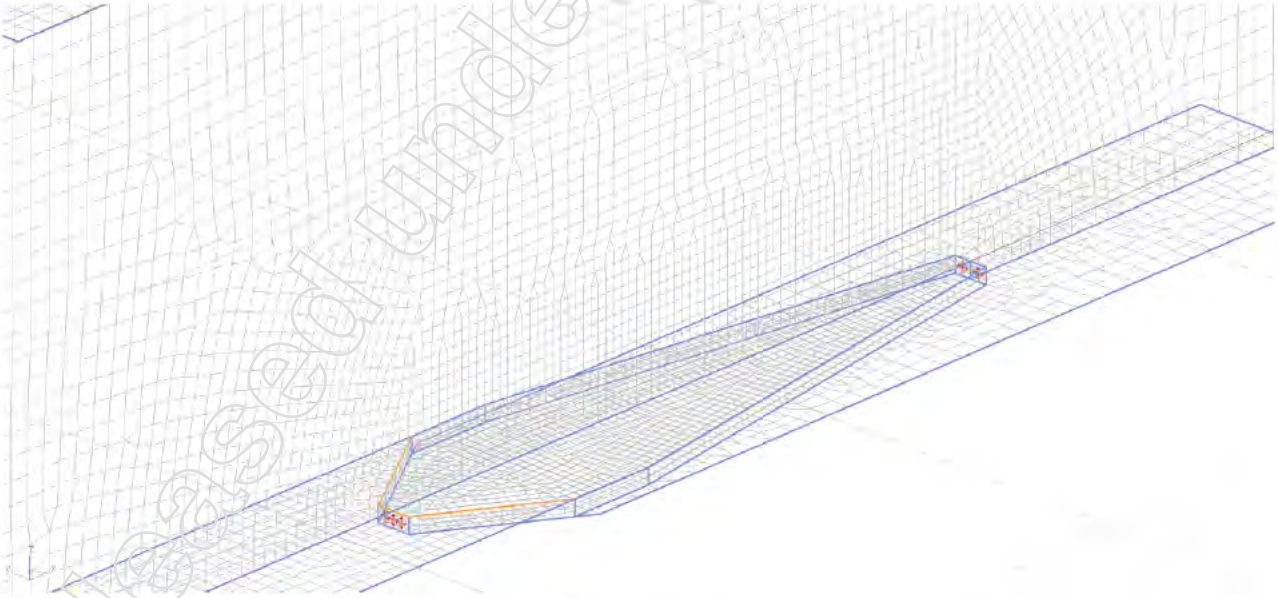

Figure 20: Detailed FE model of splice connection.

The geometry of the splice plates has been modelled with 2D shell elements at the weld location the plates are connected with shell elements with a thickness of 8.7mm.

The leg of the weld specified on the structural drawings is 3/8inch or 9.5mm. For a 45degree weld profile the throat dimension is 6.7mm. The welding process involves an amount of fusion into the parent plates and therefore the penetration at

the root exceeds the geometric throat dimension given above. 2mm of penetration at the root has been assumed which is expected to be conservative. The weld geometry assumed in shown in Figure 21.

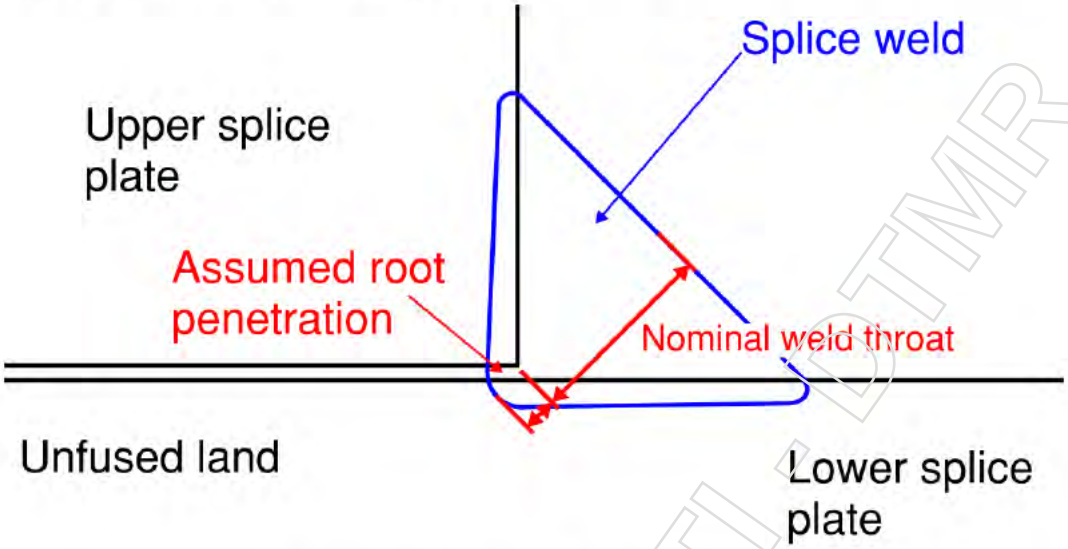

Figure 21: Assumption on geometry of splice weld

The principal stress extracted from the model is therefore determined based on the forces transferred through a stress area equivalent to the effect throat of the weld. When remedial works were undertaken in the 1960s to remove the weldment from the transverse ends of the splice plates, the remaining weld along the longitudinal edge of the splice plates was tapered, this detail can be seen in Figure 15. To account for this, the initial portion of each weld (100mm) has been tapered by reducing the thickness of each element incrementally down to 5.4mm at the start of the weld which corresponds to a reduction in the weld leg of 50%. Therefore, the stresses used in the ECA account for the weld area. Significant magnification of stress is therefore seen compared to the adjacent plate.

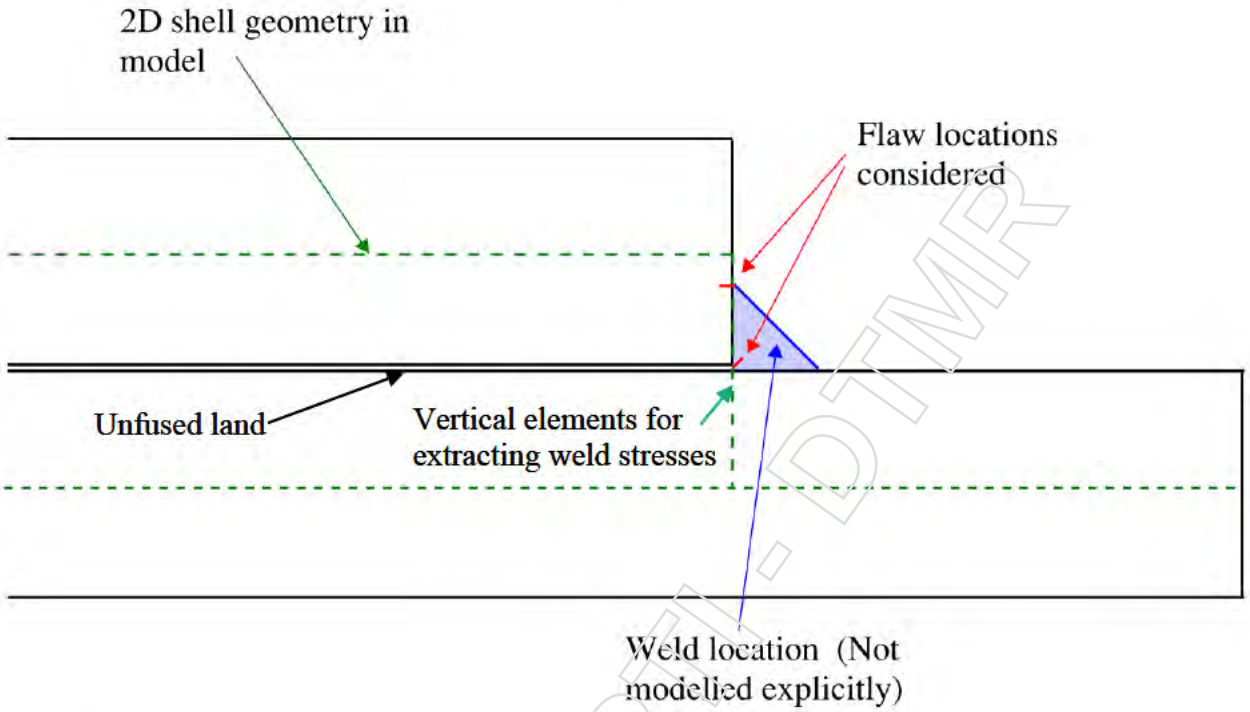

Figure 22: Graphic showing 2D model representation of splice weld detail

Figure 22 diagrammatically shows how the 2D model shown in Figure 20 relates to the actual geometry of the weld. The dotted green lines represent 2D finite elements modelled at the centreline of the flange plates. The unfused land is unconnected in the FE model. Vertical 2D elements are used to connect the flange plates at the location of the splice welds, the forces and moments passing through these elements are used to derive principal stresses at the appropriate location for the flaw being assessed. The element size and integration scheme are sufficient to appropriately characterise the stress distribution through the connection. The weld geometry itself is not modelled however the forces and moments through the weld can be calculated, and hence a principal stress can be derived for use in the ECA.

The principal stress field varies between the two flange splice plate centrelines and therefore depending on the flaw location assumed (i.e. root of toe), the stress is interpolated at the appropriate position from integration points through the height of the weld elements.

For weld defects, an Mk factor for stress magnification due to weld profile is assumed. Solutions for weld toe Mk factors have been used from Annex M of BS7910:2019. For flaws at the weld root, the same Mk factor has been applied, in conjunction with appropriate stresses at the root location, this is discussed in Section 5.2.

Grinding of priority, one cracks has resulted in loss of weld at the ends of the splice tapers. ECAs have also been conducted for the stress field seen at the toe and root of the weld at the new weld termination post-grinding. This is achieved by removing some weld elements from the local analysis model as shown in Figure 23 below. This removes connectivity between the flange splice plates

where weld has been removed and transfers load to the remaining welded connection.

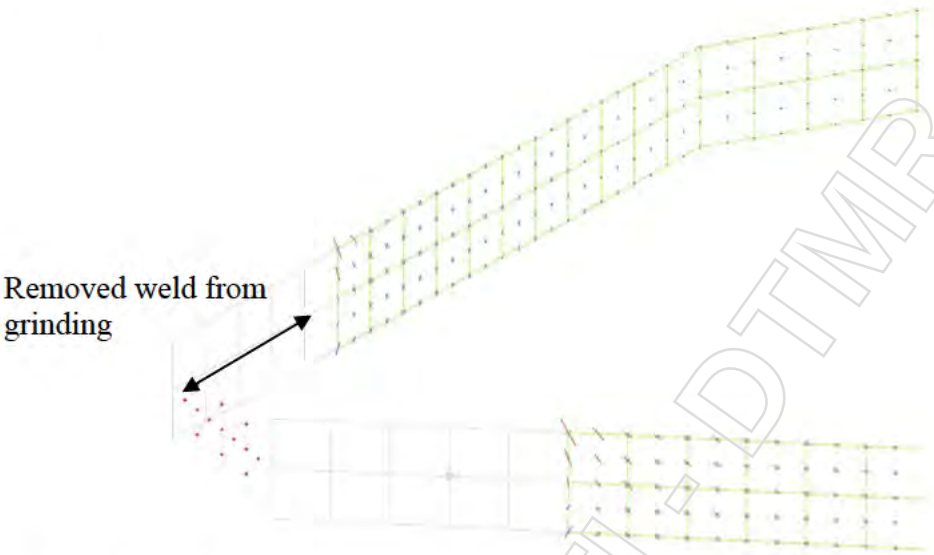

Figure 23: Weld grinding effect modelled by removing weld elements from splice taper (dummy elements).

5.3.2 Cross Girder

A detailed model including cross girder stiffeners is shown in Figure 26. Based on the evidence of cracks identified through NDT, flaws at the weld toes of fillet welded stiffeners to the web and flanges are considered. Stresses for ECA are extracted from the detailed model using a hotspot method to interpolate the stress at the location of the weld toe. Integration points at the outer surface of the 2D shell element are used.

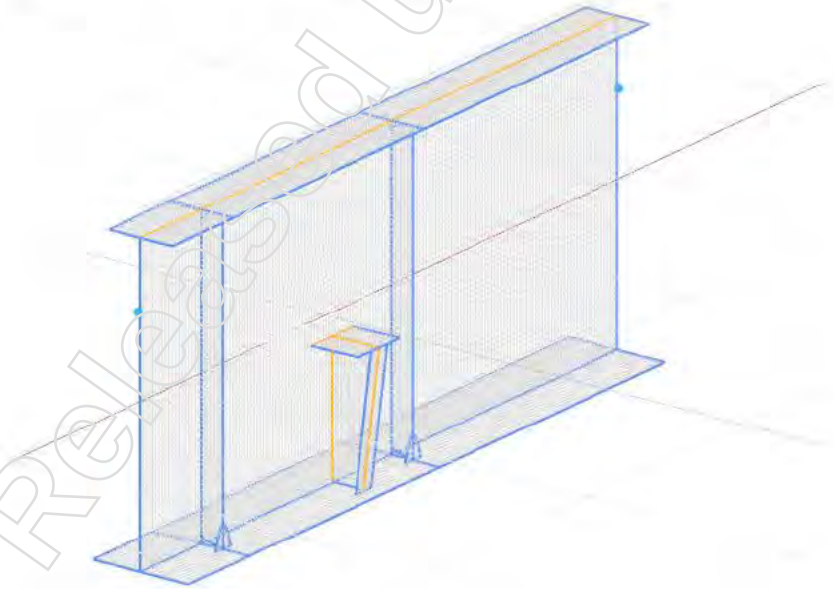

Figure 24: Detailed FE model of web stiffener/attachment.

The worst case positions on the weld has been considered for the ECA with appropriate direct stresses for Mode I opening taken. The cases considered are given in Section 5.4.3.

5.4 Primary Stresses for ECA

Primary stress (load which can contribute to plastic collapse) is extracted from the finite element models described in Section 5.3.

For the ECAs of the bottom flange splice welds, the maximum principal stress is used representing the maximum opening stress for a flaw. This is considered conservative for the crack front which varies in position and orientation through the weld.

For flaws on the cross girder stiffeners, the inspected orientation has been defects at the weld toe and therefore appropriate directional stresses relevant to Mode I tensile opening have been used.

For the bottom flange splices, stresses at both ends of the splice tapers were considered separately for the upper and lower splices in both the pre and post-grinding scenario as the geometry gives different stress distributions. This is shown in Figure 25. The lower splice tapers are typically more onerous in terms of weld stresses.

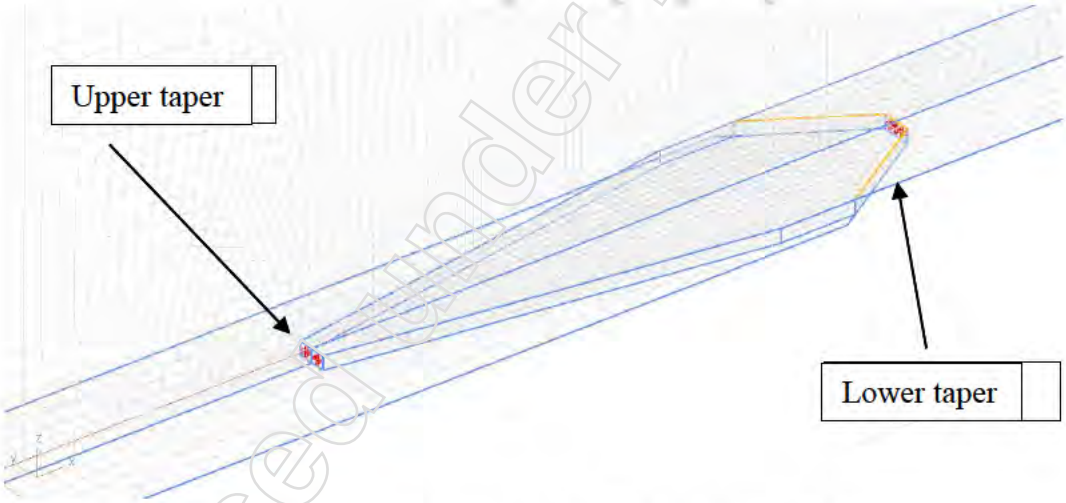

Figure 25: Consideration of splice geometry in stress extraction for ECA.

Primary stresses have been extracted for the following vehicles:

- 42.5 t 1G vehicle
- 50.5 t Truck and Dog
- 79t Crane

The vehicle position along the bridge which results in maximum stress at the flaw location for the ECA is considered for the static ECAs, the spectrum is considered for fatigue assessment in Section 6.

The stresses used for the ECAs are reported in Section 5.4.1 for the edge girder, Section 5.4.2 for the centre girder, and Section 5.4.3 for the cross girder.

5.4.1 Edge Girder (G1 and G4)

The following cases are considered for the edge girder with vehicle running directly above the girder, this represents the worst stress case for 2-lane running. Splice 2 is considered.

Cases 1 to 6 represent the weld in the unground state, pre repair. Cases 7 to 12 represent the weld in the ground state, post repair with 100mm of weld removed – The maximum weld removal that has been currently recommended.

ECA case	Vehicle	Flaw position	Taper/Splice position	Weld Pre/Post Repair Grinding[2]	Maximum Principal Stress (MPa)
1a	1G	Weld toe	Upper	Pre-Repair	43.01
1b	1G	Weld Root	Upper	Pre-Repair	9.19
2a	T+D	Weld toe	Upper	Pre-Repair	43.73
2b	T+D	Weld Root	Upper	Pre-Repair	9.33
3a	Crane	Weld toe	Upper	Pre-Repair	61.42
3b	Crane	Weld Root	Upper	Pre-Repair	12.66
4a	1G	Weld toe	Lower	Pre-Repair	58.77
4b	1G	Weld Root	Lower	Pre-Repair	70.72
5a	T+D	Weld toe	Lower	Pre-Repair	59.56
5b	T+D	Weld Root	Lower	Pre-Repair	73.03
6a	Crane	Weld toe	Lower	Pre-Repair	78.54
6b	Crane	Weld Root	Lower	Pre-Repair	114.30
7a	1G	Weld toe	Upper	Post-Repair	36.48
7b	1G	Weld Root	Upper	Post-Repair	12.10
8a	T+D	Weld toe	Upper	Post-Repair	37.12
8b	T+D	Weld Root	Upper	Post-Repair	12.27
9a	Crane	Weld toe	Upper	Post-Repair	53.02
9b	Crane	Weld Root	Upper	Post-Repair	16.53
10a	1G	Weld toe	Lower	Post-Repair	60.57
10b	1G	Weld Root	Lower	Post-Repair	62.77
11a	T+D	Weld toe	Lower	Post-Repair	61.38
11b	T+D	Weld Root	Lower	Post-Repair	64.81
12a	Crane	Weld toe	Lower	Post-Repair	81.01
12b	Crane	Weld Root	Lower	Post-Repair	101.10

Table 6 Edge girder weld maximum stresses for ECA.

[2] Post-repair accounts for 100mm of weld removed through grinding, see Section 5.3.

5.4.2

5.4.2 Internal Girder (G2 and G3)

The following cases are considered for the internal girders with vehicle running directly above an internal girder, this represents the worst stress case for centre running. Note that stresses on the edge girders are governed by vehicles above the edge girder. I.e. stresses on the edge girder from a vehicle running down the centre of the bridge are bounded from stresses from a vehicle running in the outer lane.

ECA case	Vehicle	Flaw position	Taper/Splice position	Weld Pre/Post Repair Grinding[3]	Maximum Principal Stress (MPa)
13a	1G	Weld toe	Upper	Pre-Repair	24.13
13b	1G	Weld Root	Upper	Pre-Repair	5.67
14a	T+D	Weld toe	Upper	Pre-Repair	24.53
14b	T+D	Weld Root	Upper	Pre-Repair	5.744
15a	Crane	Weld toe	Upper	Pre-Repair	36.27
15b	Crane	Weld Root	Upper	Pre-Repair	7.838
16a	1G	Weld toe	Lower	Pre-Repair	41.21
16b	1G	Weld Root	Lower	Pre-Repair	35.96
17a	T+D	Weld toe	Lower	Pre-Repair	41.67
17b	T+D	Weld Root	Lower	Pre-Repair	35.39
18a	Crane	Weld toe	Lower	Pre-Repair	54.64
18b	Crane	Weld Root	Lower	Pre-Repair	64.07
19a	1G	Weld toe	Upper	Post-Repair	20.48
19b	1G	Weld Root	Upper	Post-Repair	7.84
20a	T+D	Weld toe	Upper	Post-Repair	20.85
20b	T+D	Weld Root	Upper	Post-Repair	7.933
21a	Crane	Weld toe	Upper	Post-Repair	32.05
21b	Crane	Weld Root	Upper	Post-Repair	10.76
22a	1G	Weld toe	Lower	Post-Repair	45.18
22b	1G	Weld Root	Lower	Post-Repair	33.9
23a	T+D	Weld toe	Lower	Post-Repair	45.69
23b	T+D	Weld Root	Lower	Post-Repair	33.19
24a	Crane	Weld toe	Lower	Post-Repair	59.98
24b	Crane	Weld Root	Lower	Post-Repair	59.71

Table 7 Internal girders, weld maximum stresses for ECA.

In the previously reported preliminary ECAs, stresses at the weld defect were estimated by applying a stress concentration factor to member stresses from the global model. The more accurate stresses obtained from detailed finite element

[3] Post-repair accounts for 100mm of weld removed through grinding, see Section 05.3.

modelling show that the preliminary assessment bounded the most severe defect positions, but for many defects were conservative.

5.4.3 Cross Girders

A single worst-case position has been considered for welded attachments to the cross girder webs and bottom flanges as indicated in Figure 26. Given that the cross girders are located at multiple locations across the span of the bridge and that attachments also occur at different locations, additional ECAs are presented at 50% and 75% of the 1G vehicle load to enable interpolation of the results for cross girders or attachments not located in the most onerous span position.

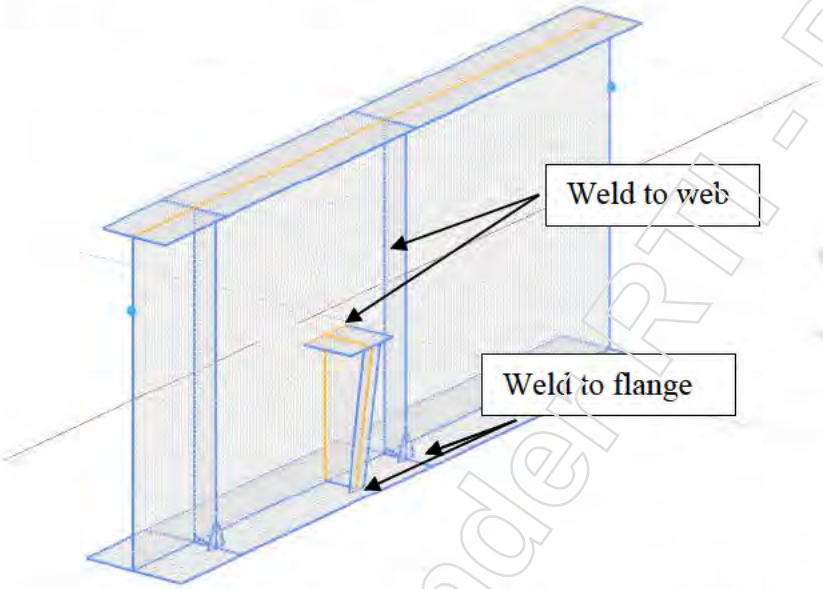

Figure 26: Weld locations considered for Cross Girder stiffeners.

ECA case	Vehicle	Flaw position	Member Considered	Maximum Stress (MPa)
25	1G	Weld toe	Web	32.19
26	T+D	Weld toe	Web	33.28
27	Crane	Weld toe	Web	53.35
28	1G	Weld toe	Flange	64.45
29	T+D	Weld toe	Flange	66.20
30	Crane	Weld toe	Flange	97.14

Table 8 Cross girder web attachment maximum stresses for ECA.

5.5 Secondary (Residual) Stress

The main sources for residual (self-equilibrating) stress in the critical details will be from welding when the girders were fabricated. Secondary stresses have

significant influence on crack tip stress conditions and also influences the fatigue stress range as discussed in Section 6.1.

Differential cooling and constraint during welding causes areas of localised stress distributions which can reach the yield strength of the steel in tension. Yield magnitude residual stresses are typically largest at the surface of the plate, and decay through thickness. The residual stresses are self-equilibrating and do not contribute to plastic collapse, i.e. in the ECA secondary stress contributes to the fracture ratio (Kr) but not the load ratio (Lr).

Relaxation of residual stresses can be achieved through interventions such as post weld heat treatment or compression peening, it can also occur through elastic shakedown. Several plastic load cycles at the start of component service relaxes the residual stress distribution, with further service remaining elastic, however the stress history of the structure is not known.

Where flaws are present in the structure, relaxation of secondary stresses can occur local to the crack tip if the magnitude of crack tip reference stress is sufficiently high. In the case of flaws in the splice plate welds, the applied primary stresses tabulated in Section 5.4.1 and 5.4.2 not typically not sufficient to result in relaxation according to equations 7.24a and 7.24b in BS 7910:2019 based on the relevant reference stress solutions for the flaws considered, however relaxation is considered in the ECAs.

Therefore, yield magnitude residual stress has been assumed to act in tension for the ECAs presented in this report for defects in the weld metal or HAZ.

5.6 Defect Orientation

Defects are assumed oriented perpendicular to the principal stress acting in the structure at the defect location. I.e. the tensile stresses used in the ECA are assumed to be opening the defects in mode I.

5.7 Engineering Critical Assessment

A series of option 1 ECAs have been conducted to BS 7910:2019 to determine critical flaw sizes for the loading and defect scenarios described in Sections 5.4.1, 5.4.2, and 5.4.3. These are presented in Sections 5.7.1, 5.7.2, 5.7.3 for flaws in the edge and internal girders (G1 to G4) and Section 5.7.4 for flaws in the cross girders.

The ECAs are summarised as follows to assist with the interpretation of flaws identified on the structure which is further discussed in Section 8.

ECAs are presented as follows for the flaw characterisations discussed in Section 5.2.

For the weld toe flaws in the bottom flange splice welds, type 1 flaws:

1. Critical flaw dimensions for aspect ratio a/2c=0.025, 0.1, and 0.4.
2. Graph showing critical flaw height against length for typical flaw lengths, this shows the critical flaw dimensions for a range of flaw lengths.

These ECAs are reported in Section 5.7.1.

For weld root defects in the bottom flange splice welds before grinding, type 2a flaws:

1. The critical length of through thickness flaws at the start of the weld is determined

These ECAs are reported in Section 5.7.2.

For weld root defects in the bottom flange splice welds after grinding, type 2b flaws:

1. Critical flaw dimensions for aspect ratio a/2c=0.025, 0.1, and 0.4.
2. Graph showing critical flaw height against length for typical flaw lengths, this shows the critical flaw dimensions for a range of flaw lengths.

These ECAs are reported in Section 5.7.3.

For weld toe flaws in the cross girder stiffener welds:

1. Critical flaw dimensions for aspect ratio a/2c=0.025, 0.1, and 0.4.
2. Graph showing critical flaw height against length for typical flaw lengths, this shows the critical flaw dimensions for a range of flaw lengths.

The ECAs for flaws in the flange plates are reported in Sections 5.7.1, 5.7.2 & 5.7.3 and for cross girder defects in Section 5.7.4.

5.7.1 Edge and Internal Girder bottom flange splice welds, toe defects (Type 1 flaws)

Option 1 ECAs have been conducted for flaws characterised as type 2a1 flaws in Section 5.2.1.1.

For the edge girders, applied primary stress is according to case numbers in Table 6. In the tables, the critical flaw height, a_{crit} refers to the depth of the flaw as measured with NDT. The length, 2c, refers to the length of defect at the surface.

The critical flaw dimensions are shown in Table 9 for weld toe defects in the edge girder pre-grinding, i.e. without repair at the original tapered weld locations.

ECA case	Vehicle	Taper/Splice position	Aspect Ratio a/2c (0.025)		Aspect Ratio a/2c (0.1)		Aspect Ratio a/2c (0.4)	
			acrit (mm)	2c (mm)	acrit (mm)	acrit (mm)	2c (mm)	acrit (mm)
1a	1G	Upper	2.7	108	3.1	31	5.3	13.3
2a	T+D	Upper	2.7	108	3.1	31	5.3	13.3
3a	Crane	Upper	2.3	92	2.7	27	4.2	10.5
4a	1G	Lower	2.4	96	2.7	27	4.4	17.6

ECA case	Vehicle	Taper/Splice position	Aspect Ratio a/2c (0.025)		Aspect Ratio a/2c (0.1)		Aspect Ratio a/2c (0.4)	
			acrit (mm)	2c (mm)	acrit (mm)	acrit (mm)	2c (mm)	acrit (mm)
5a	T+D	Lower	2.4	96	2.7	27	4.3	10.8
6a	Crane	Lower	2.0	80	2.3	23	3.5	8.8

Table 9 Critical flaw dimensions for type 1 defects at weld toe of edge girder bottom flange splice welds pre-grinding.

The critical flaw dimensions are shown in Table 10 for weld toe defects in the edge girders post-grinding, i.e. After up to 100mm of weld has been removed from the original weld.

ECA case	Vehicle	Taper/Splice position	Aspect Ratio a/2c (0.025)		Aspect Ratio a/2c (0.1)		Aspect Ratio a/2c (0.4)	
			acrit (mm)	2c (mm)	acrit (mm)	acrit (mm)	2c (mm)	acrit (mm)
7a	1G	Upper	2.9	116	3.3	33	5.8	14.5
8a	T+D	Upper	2.9	116	3.2	32	5.7	14.3
9a	Crane	Upper	2.5	100	2.9	29	4.7	11.8
10a	1G	Lower	2.4	96	2.7	27	4.3	10.8
11a	T+D	Lower	2.3	92	2.7	27	4.2	10.5
12a	Crane	Lower	2.0	80	2.3	23	3.4	8.5

Table 10 Critical flaw dimensions for type 1 defects at weld toe of edge girder bottom flange splice welds post-grinding.

For the internal girder, applied primary stress is according to case numbers in Table 7Table 6. In the tables, the critical flaw height, a_{crit} refers to the depth of the flaw as measured with NDT. The length, 2c, refers to the length of defect at the surface.

The critical flaw dimensions are shown in Table 9 for weld toe defects in the internal girder pre-grinding, i.e. without repair at the original tapered weld location.

ECA case	Vehicle	Taper/Splice position	Aspect Ratio a/2c (0.025)		Aspect Ratio a/2c (0.1)		Aspect Ratio a/2c (0.4)	
			a_{crit} (mm)	2c (mm)	a_{crit} (mm)	a_{crit} (mm)	2c (mm)	a_{crit} (mm)
13a	1G	Upper	3.5	140	3.6	78	6.8	17
14a	T+D	Upper	3.2	128	3.6	36	6.8	17
15a	Crane	Upper	2.9	116	3.3	33	5.8	14.5
16a	1G	Lower	2.8	112	3.2	32	5.5	13.8
17a	T+D	Lower	2.8	112	3.1	31	5.4	13.5
18a	Crane	Lower	2.5	100	2.8	28	4.6	11.5

Table 11 Critical flaw dimensions for type 1 defects at weld toe of internal girder bottom flange splice welds pre-grinding.

The critical flaw dimensions are shown in Table 10 for weld toe defects in the internal girder post-grinding, i.e. After up to 100mm of weld has been removed from the original weld.

ECA case	Vehicle	Taper/Splice position	Aspect Ratio a/2c (0.025)		Aspect Ratio a/2c (0.1)		Aspect Ratio a/2c (0.4)	
			a_{crit} (mm)	2c (mm)	a_{crit} (mm)	a_{crit} (mm)	2c (mm)	a_{crit} (mm)
19a	1G	Upper	3.2	128	3.6	36	6.8	17
20a	T+D	Upper	3.3	132	3.7	37	7.1	17.8
21a	Crane	Upper	3.0	150	3.4	34	6.1	15.3
22a	1G	Lower	2.7	108	3.0	30	5.2	13
23a	T+D	Lower	2.7	108	3.0	30	5.1	12.8
24a	Crane	Lower	2.4	96	2.7	27	4.3	10.8

Table 12 Critical flaw dimensions for type 1 defects at weld toe of internal girder bottom flange splice welds post-grinding.

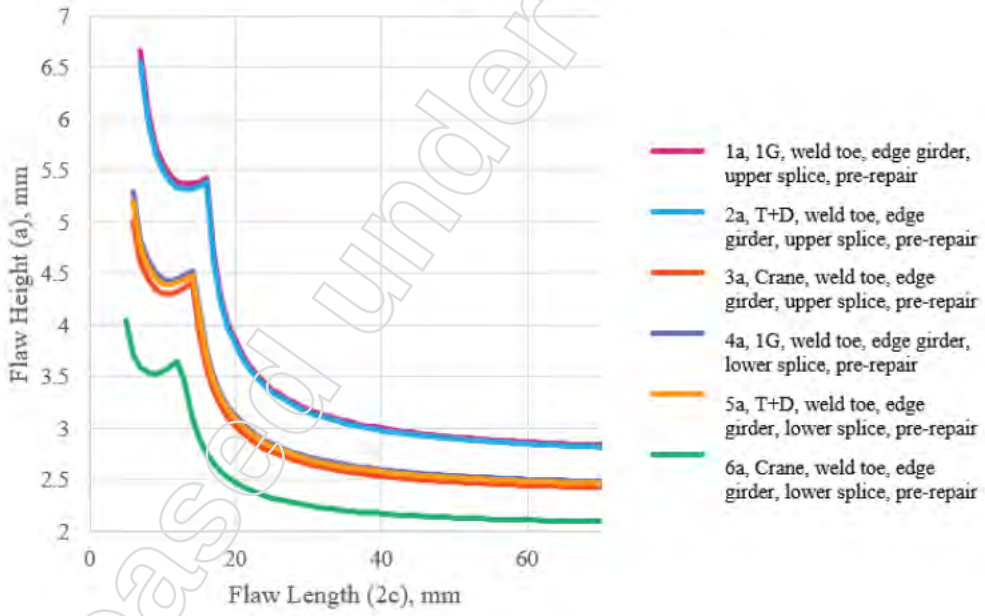

Figure 27: Critical flaw height versus length for flaws at the weld toe of edge girder, bottom flange splice welds before repair/grinding. Upper and lower splices shown for all vehicles.

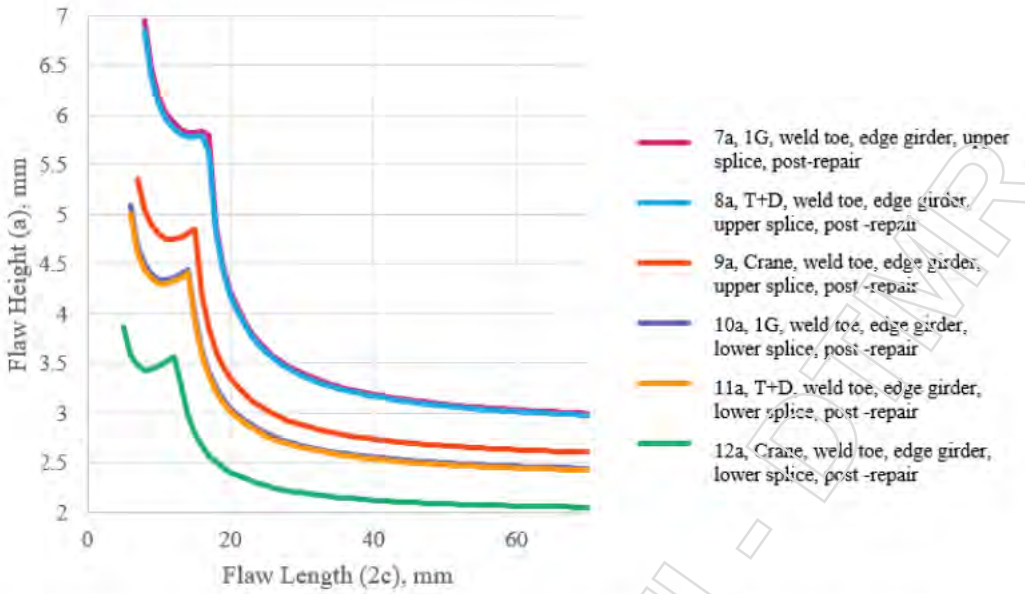

Figure 28: Critical flaw height versus length for flaws at the weld toe of edge girder, bottom flange splice welds after repair/grinding of 100mm of weld. Upper lower splices shown for all vehicles.

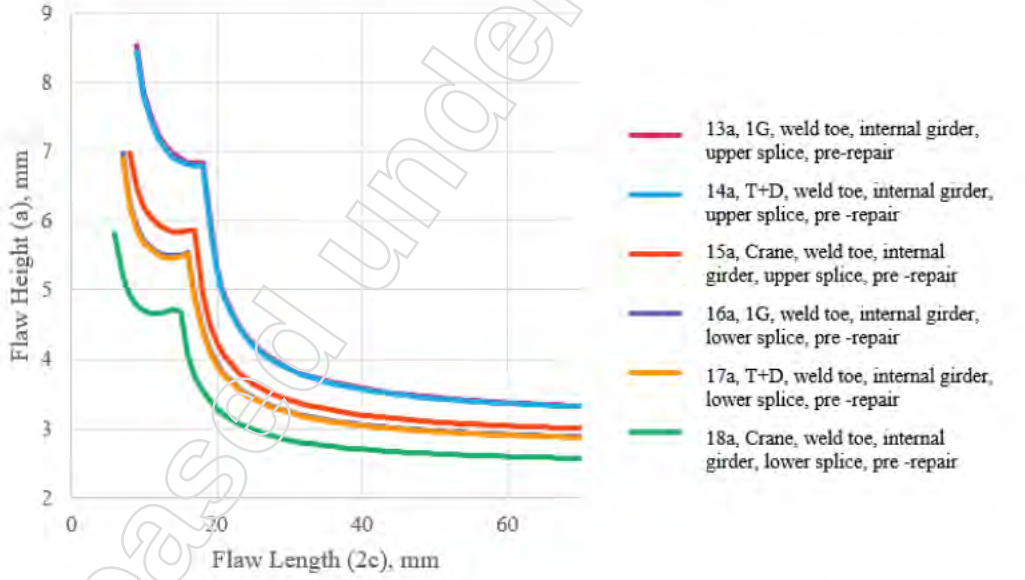

Figure 29: Critical flaw height versus length for flaws at the weld toe of internal girder, bottom flange splice welds before repair/grinding. Upper lower splices shown for all vehicles.

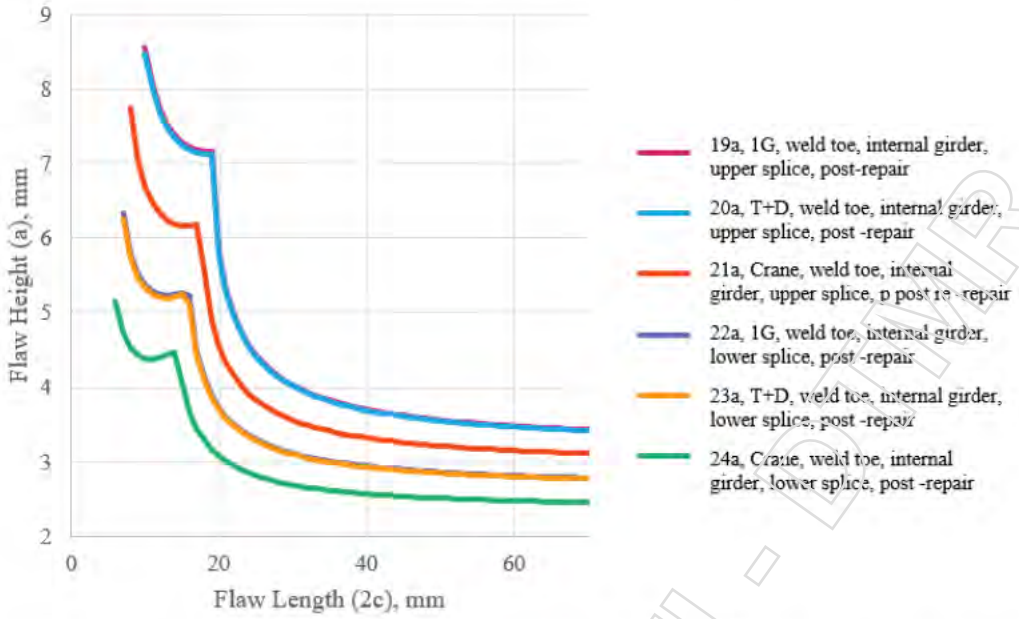

Figure 30: Critical flaw height versus length for flaws at the weld toe of internal girder, bottom flange splice welds after repair/grinding of 100mm of weld. Upper lower splices shown for all vehicles.

5.7.2 Bottom flange splice welds, root defects pre-grinding (Type 2a flaws)

Option 1 ECAs have been conducted for flaws characterised as type 2a flaws in Section 5.2.1.2

For the edge girder, applied primary stress is according to case numbers in Table 6. The critical flaw lengths, i.e. the maximum safe length of flaw that can be seen at the surface of the weld is shown in Table 13.

ECA case	Vehicle	Taper/Splice position	Critical flaw length, $2c_{crit}$ (mm)
1b	1G	Upper	9.5
2b	T+D	Upper	9.5
3b	Crane	Upper	9.2
4b	1G	Lower	5.7
5b	T+D	Lower	5.6
6b	Crane	Lower	4.0

Table 13 Critical flaw lengths at weld throat surface for type 2a defects in edge girder bottom flange splice welds.

For the internal girder, applied primary stress is according to case numbers in Table 7. The critical flaw lengths, i.e. the maximum safe length of flaw that can be seen at the surface of the weld is shown in Table 14.

ECA case	Vehicle	Taper/Splice position	Critical flaw length, $2c_{crit}$ (mm)
13b	1G	Upper	9.8
14b	T+D	Upper	9.8
15b	Crane	Upper	9.6
16b	1G	Lower	7.6
17b	T+D	Lower	7.6
18b	Crane	Lower	6.0

Table 14 Critical flaw lengths at weld throat surface for type 2a defects in edge girder bottom flange splice welds.

5.7.3 Bottom flange splice welds, root defects post-grinding (Type 2b flaws)

In Table 15 below, a_{crit} refers to the critical flaw height for the assumed flaw length (2c). The flaw height, a, is the dimension of the exposed root defect that would be identified during NDT of the residual root flaw. Note that flaw heights are considered in 0.1mm increments.

For the edge girder, applied primary stress is according to case numbers in Table 6.

ECA case	Vehicle	Taper/Splice position	Aspect Ratio a/2c (0.005)		Aspect Ratio a/2c (0.025)		Aspect Ratio a/2c (0.1)	
			a_{crit} (mm)	2c (mm)	a_{crit} (mm)	2c (mm)	a_{crit} (mm)	2c (mm)
7b	1G	Upper	2.2	440	2.4	96	2.9	29
8b	T+D	Upper	2.2	440	2.4	96	2.9	29
9b	Crane	Upper	2.1	420	2.3	92	2.8	28
10b	1G	Lower	1.7	340	1.8	72	2.1	21
11b	T+D	Lower	1.7	340	1.8	72	2.1	21
12b	Crane	Lower	1.3	260	1.4	56	1.6	16

Table 15 Critical flaw heights at exposed weld face post-grinding for type 2b defects in edge girder bottom flange splice welds.

For the internal girder, applied primary stress is according to case numbers in Table 7.

ECA case	Vehicle	Taper/Splice position	Aspect Ratio a/2c (0.005)		Aspect Ratio a/2c (0.025)		Aspect Ratio a/2c (0.1)	
			a_{crit} (mm)	2c (mm)	a_{crit} (mm)	2c (mm)	a_{crit} (mm)	2c (mm)
19b	1G	Upper	2.2	440	2.4	96	3.0	30
20b	T+D	Upper	2.2	440	2.4	96	3.0	30
21b	Crane	Upper	2.2	440	2.4	96	2.9	29
22b	1G	Lower	2.0	400	2.1	84	2.6	26

ECA case	Vehicle	Taper/Splice position	Aspect Ratio a/2c (0.005)		Aspect Ratio a/2c (0.025)		Aspect Ratio a/2c (0.1)	
			a_{crit} (mm)	2c (mm)	a_{crit} (mm)	2c (mm)	a_{crit} (mm)	2c (mm)
23b	T+D	Lower	2.0	400	2.1	84	2.6	26
24b	Crane	Lower	1.7	340	1.8	72	2.2	22

Table 16 Critical flaw heights at exposed weld face post-grinding for type 2b defects in internal girder bottom flange splice welds.

The following figure shows the sensitivity of critical flaw height to flaw length along the remaining weld root. As the length of the remaining defect is difficult to detect, these charts show the acceptable residual flaw height for long residual defects.

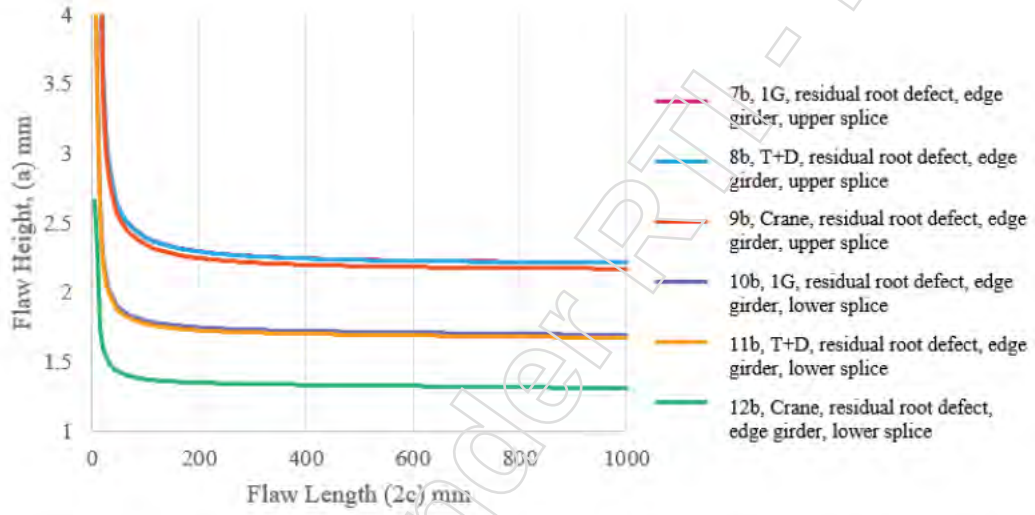

Figure 31: Edge girder, critical flaw height versus flaw length for residual root defects after grinding.

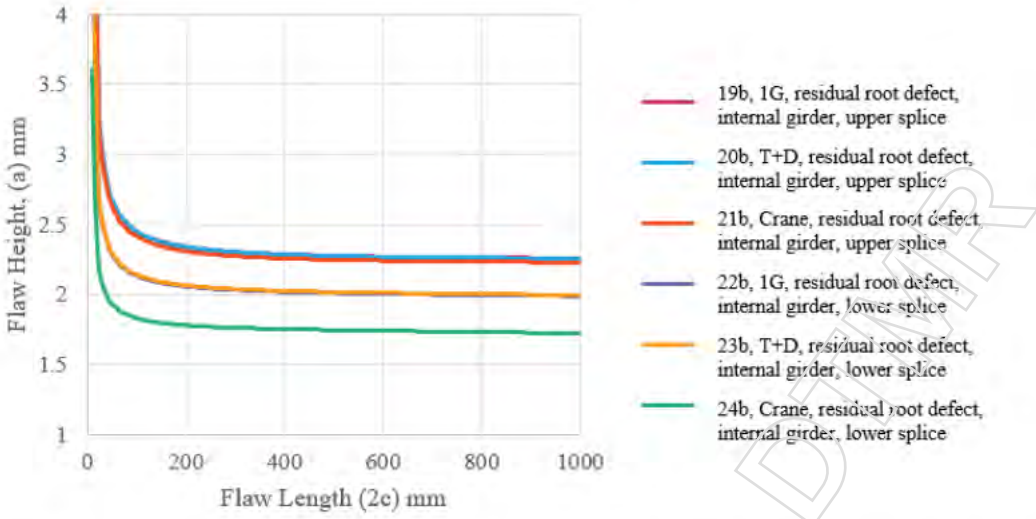

Figure 32: Internal girder, critical flaw height versus flaw length for residual root defects after grinding.

5.7.4 Cross Girder defects

Option 1 ECAs have been conducted for cross girder flaws characterised as in Section 5.2.2.

For the cross girder, applied primary stress is according to case numbers in Table 8 Table 6.

In the tables, the critical flaw height, a_{crit} refers to the depth of the flaw as measured with NDT. The length, 2c, refers to the length of defect at the surface.

ECA case	Vehicle	Aspect Ratio a/2c (0.025)		Aspect Ratio a/2c (0.1)		Aspect Ratio a/2c (0.4)	
		a_{crit} (mm)	2c (mm)	a_{crit} (mm)	a_{crit} (mm)	2c (mm)	a_{crit} (mm)
25a	1G	4.3	172	4.8	48	9.1	22.8
25b	50% 1G load	4.6	184	5.9	59	10.3	25.8
25c	75% 1G load	4.4	176	5.7	57	9.7	24.3
26	T+D	5.1	204	6.7	67	10.7	26.8
27	Crane	4.7	188	6.2	62	6.2	15.5

Table 17 Critical flaw dimensions for flaws at the weld toe of attachments to the cross girder webs.

ECA case	Vehicle	Aspect Ratio a/2c (0.025)		Aspect Ratio a/2c (0.1)		Aspect Ratio a/2c (0.4)	
		a_{crit} (mm)	2c (mm)	a_{crit} (mm)	a_{crit} (mm)	2c (mm)	a_{crit} (mm)
28a	1G	1.9	76	2.2	22	3.2	8
28b	50% 1G load	2.4	96	2.9	29	4.8	12
28c	75% 1G load	2.1	84	2.5	25	3.9	10
29	T+D	1.9	76	2.2	22	3.1	8
30	Crane	1.4	56	1.7	17	2.2	5.5

Table 18 Critical flaw dimensions for flaws at the weld toe of attachments to the cross girder webs.

The following figures shows the sensitivity of critical flaw height to flaw length for flaws at the toe of stiffener welds on the cross girders.

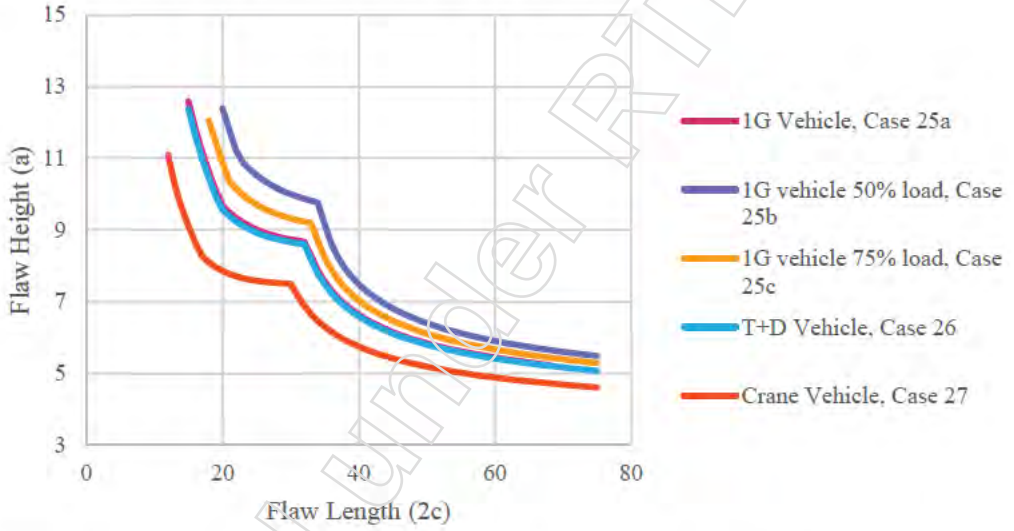

Figure 33: Critical flaw height versus length for flaws at the weld toe of connections to the cross girder web.

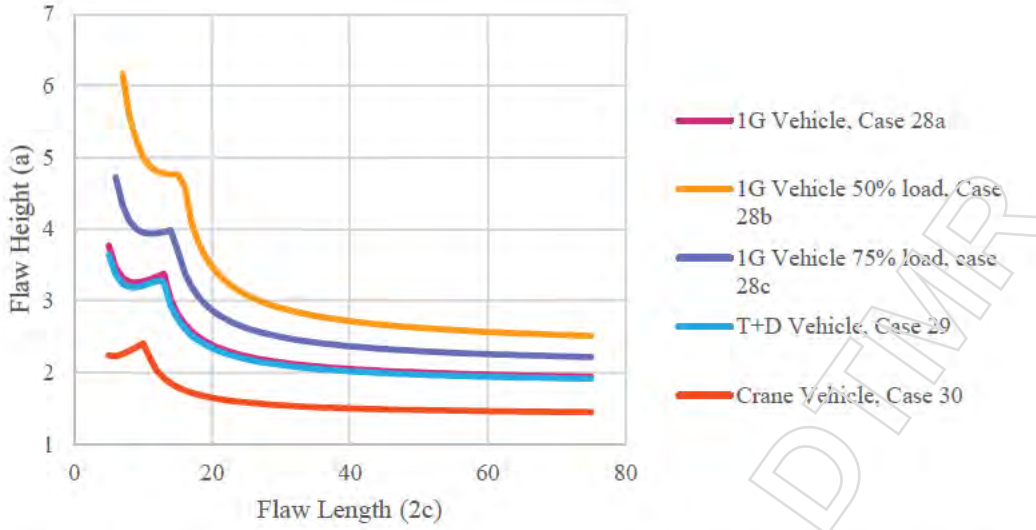

Figure 34: Critical flaw height versus length for flaws at the weld toes of connections to the bottom flange of cross girders.

5.8 Summary

The ECAs presented demonstrate the following:

The edge girders (G1 and G4) are more highly stressed and more critical to brittle fracture than the centre girders (G2 and G3).

The short ends of the lower splices are more highly stressed than the long ends of the upper splices and more critical to brittle fracture.

For defects at the weld toe of stiffeners welded to the cross girder bottom flange, the critical flaw dimensions are below typical detection capabilities of MPI in the as welded condition. Enhanced NDT is likely to be required for these details which may include: Improving surface finish or increasing the sensitivity of the MPI system such that the required defect size can be detected. Alternatively, toe grinding of the stiffener welds could be considered to remove potential defects and improve the fatigue performance of the welds.

For bottom flange splice welds on the edge and internal girders which have not been repaired by grinding, the critical length of though thickness flaws is found to be small. For the short dimension of splice plate, the critical length under loading from the crane vehicle on the edge girder is shorter that the length sizing error MPI inspection, therefore cranes should not be run in the outer lanes. Generally, the critical length of this defect type is sufficiently small that it is recommended that any flaw visible at the surface of the splice welds, as shown in Figure 15, should be removed by grinding as previously done for priority 1 defects.

After grinding, the critical height of the residual root defect is small, between 1.3mm and 2.2mm height. These flaw heights are difficult to detect and the length of flaw is unlikely to be reliably determined. Crane vehicles should not be run in the outer lane and this. This restriction increases the minimum critical flaw height to 1.7mm.

If the height of the residual defect cannot be reliably determined then the risk of fracture can only be reduced by repair of the ground out weld material to reduce the stress caused by removal, or speed reduction of vehicles to decrease the magnitude of loads on the connections.

Two lane running of 1G and T+D vehicles is subject to the NDT capabilities employed on the structure.

6 Fatigue

The ECAs presented in Section 5 present critical flaw dimension for weld toe and root defects in the girder bottom flange splice details and at welds between stiffeners and the cross girder flanges and webs. These critical flaw dimensions are also presented in terms of critical flaw depth versus length to show the effect of flaw aspect ratio on risk of brittle fracture.

The ECAs presented in Section 5.7 do not account for cyclic loading on the bridge from vehicle traffic growing the cracks incrementally over time. They represent critical dimensions of a flaw in the structure, that when reached poses a risk of failure. Given the repetitive loading from vehicles which leads to fluctuating stresses in the splice connections, the following calculations predict the growth of flaws with cyclic loading.

Fatigue crack growth calculations have been made using the following assumptions:

- BS7910 crack growth properties are assumed for ferritic steels, in air (non-marine)
- A stress ratio accounting for the weld is assumed
- Principal stresses are assumed to act on flaws aligned with the principal stress plane.
- 180 vehicles per day are assumed, however the no. cycles can be used to assess the flaw growth for any number of vehicles per day.

The initial defect assumed is that which could be reliably be detected by surface MPI with 2mm depth threshold. The corresponding length (which is typically recorded during inspection) accounts for sizing uncertainty according to annex T of BS7910.

Note that the results presented in Section 5.7 in some cases find critical flaw dimensions which are smaller than the proposed threshold for considering fatigue growth. Where defects are identified already exceeding the critical dimension there is a risk of failure and there is no safe remaining fatigue life, these flaws must be addressed urgently.

6.1 Fatigue Stresses

For the fatigue assessments, stress spectra are derived from the finite element models discussed in Sections 4 and0. 5.3. As a vehicle moves over the bridge, the stress at the flaw location varies as shown in Figure 35. The stress range extracted from the models typically includes a tensile portion and a compressive portion of the cycle. For flaws located in the weldment or HAZ, and subjected to tensile yield magnitude residual stress, the full stress range must be considered as damaging. The effect of superposing the fatigue stress on the residual stress is illustrated in Figure 36.

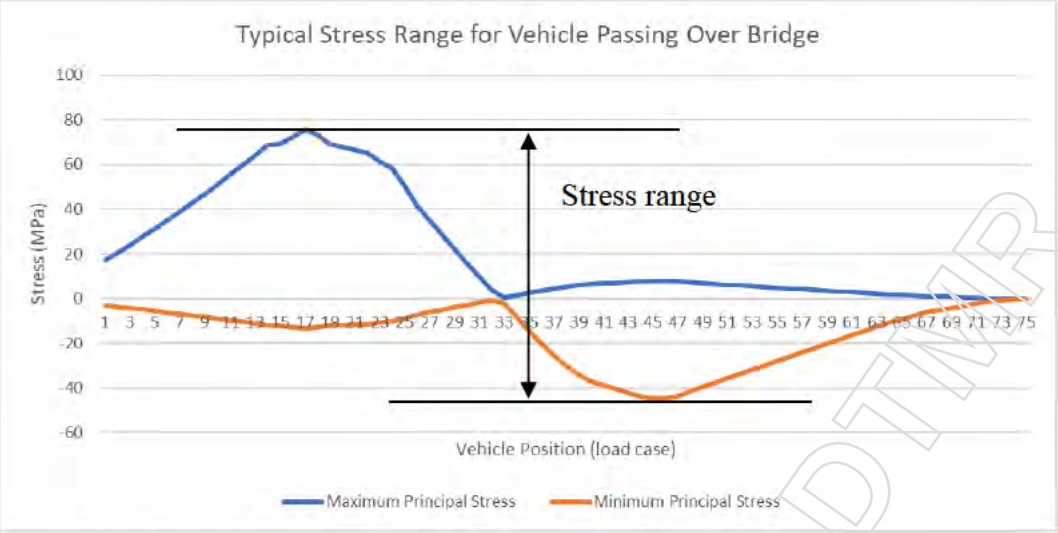

Figure 35: Typical stress range for fatigue calculation

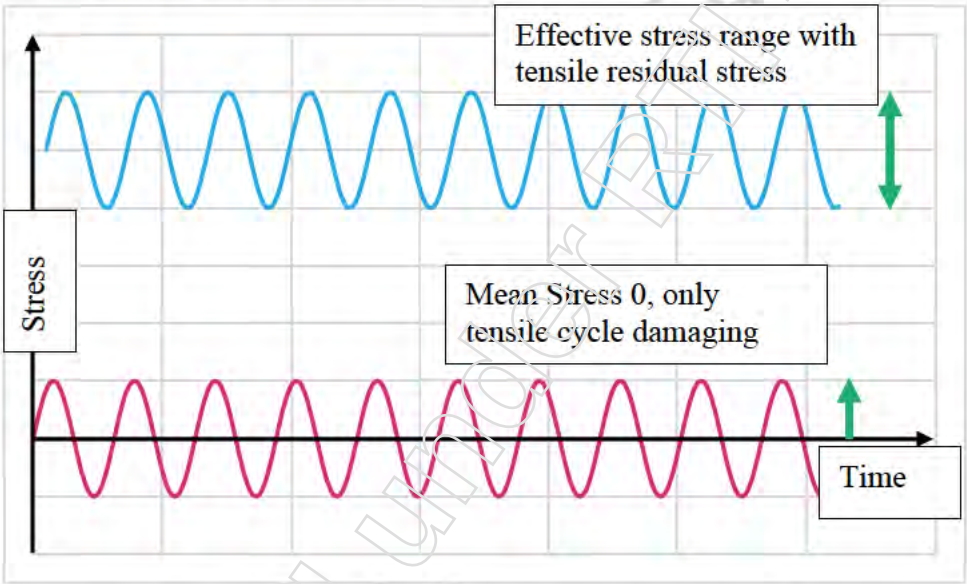

Figure 36: Effect of tensile residual stress on damaging portion of stress cycles.

The stress ranges used for the fatigue estimates are presented in the sections below, the same scenarios are cases are used as for the ECAs presented in Sections 5.4.1, 5.4.2, and 5.4.3. The static stresses from these sections are used to determine the criticality of the growing flaw, as the flaw is grown under fatigue loading in the fatigue ECA assessment.

6.1.1 Edge Girders (G1 and G4)

Fatigue ECA case	Vehicle	Flaw position	Splice geometry	Weld Pre/Post Repair Grinding[4]	Fatigue Stress Range (MPa)
1a	1G	Weld toe	Upper	Pre-Repair	134.08
1b	1G	Weld Root	Upper	Pre-Repair	24.49
2a	T+D	Weld toe	Upper	Pre-Repair	137.23
2b	T+D	Weld Root	Upper	Pre-Repair	25.06
3a	Crane	Weld toe	Upper	Pre-Repair	196.22
3b	Crane	Weld Root	Upper	Pre-Repair	35.84
4a	1G	Weld toe	Lower	Pre-Repair	125.75
4b	1G	Weld Root	Lower	Pre-Repair	132.22
5a	T+D	Weld toe	Lower	Pre-Repair	128.74
5b	T+D	Weld Root	Lower	Pre-Repair	135.36
6a	Crane	Weld toe	Lower	Pre-Repair	186.94
6b	Crane	Weld Root	Lower	Pre-Repair	196.66
7a	1G	Weld toe	Upper	Post-Repair	124.95
7b	1G	Weld Root	Upper	Post-Repair	30.78
8a	T+D	Weld toe	Upper	Post-Repair	127.85
8b	T+D	Weld Root	Upper	Post-Repair	31.49
9a	Crane	Weld toe	Upper	Post-Repair	182.52
9b	Crane	Weld Root	Upper	Post-Repair	45.14
10a	1G	Weld toe	Lower	Post-Repair	130.34
10b	1G	Weld Root	Lower	Post-Repair	116.21
11a	T+D	Weld toe	Lower	Post-Repair	133.44
11b	T+D	Weld Root	Lower	Post-Repair	118.97
12a	Crane	Weld toe	Lower	Post-Repair	193.71
12b	Crane	Weld Root	Lower	Post-Repair	172.79

Table 19 Edge girder weld maximum fatigue stress range for ECA.

6.1.2 Internal Girders (G2 and G3)

The following cases are considered for the centre girders with vehicle running directly above the girder, this represents the worst stress case for centre running. Note that stresses on the edge girders are governed by vehicles above the edge girder. I.e. stresses on the edge girder from a vehicle running down the centre of the bridge are bounded from stresses from a vehicle running in the outer lane.

[4] Post-repair accounts for 100mm of weld removed through grinding, see Section 05.3.

Fatigue ECA case	Vehicle	Flaw position	Splice geometry	Weld Pre/Post Repair Grinding[5]	Fatigue Stress Range (MPa)
13a	1G	Weld toe	Upper	Pre-Repair	79.31
13b	1G	Weld Root	Upper	Pre-Repair	14.433
14a	T+D	Weld toe	Upper	Pre-Repair	73.37
14b	T+D	Weld Root	Upper	Pre-Repair	13.672
15a	Crane	Weld toe	Upper	Pre-Repair	114.78
15b	Crane	Weld Root	Upper	Pre-Repair	20.878
16a	1G	Weld toe	Lower	Pre-Repair	76.29
16b	1G	Weld Root	Lower	Pre-Repair	77.62
17a	T+D	Weld toe	Lower	Pre-Repair	76.04
17b	T+D	Weld Root	Lower	Pre-Repair	77.52
18a	Crane	Weld toe	Lower	Pre-Repair	117.18
18b	Crane	Weld Root	Lower	Pre-Repair	73.523
19a	1G	Weld toe	Upper	Post-Repair	79.21
19b	1G	Weld Root	Upper	Post-Repair	18.996
20a	T+D	Weld toe	Upper	Post-Repair	72.03
20b	T+D	Weld Root	Upper	Post-Repair	18.083
21a	Crane	Weld toe	Upper	Post-Repair	113.03
21b	Crane	Weld Root	Upper	Post-Repair	27.64
22a	1G	Weld toe	Lower	Post-Repair	84.3
22b	1G	Weld Root	Lower	Post-Repair	71.82
23a	T+D	Weld toe	Lower	Post-Repair	83.92
23b	T+D	Weld Root	Lower	Post-Repair	71.54
24a	Crane	Weld toe	Lower	Post-Repair	129.34
24b	Crane	Weld Root	Lower	Post-Repair	110.26

Table 20 Internal girder weld maximum fatigue stress range for ECA.

6.1.3 Cross Girders

A single worst-case position has been considered for welded attachments to the cross girder webs and bottom flanges as indicated in Section 5.4.3.

Fatigue ECA case	Vehicle	Flaw position	Member Considered	Fatigue Stress Range (MPa)
25	1G	Weld toe	Web	55.52
26	T+D	Weld toe	Web	56.92
27	Crane	Weld toe	Web	84.15
28	1G	Weld toe	Flange	85.25

[5] Post-repair accounts for 100mm of weld removed through grinding, see Section 05.3.

Fatigue ECA case	Vehicle	Flaw position	Member Considered	Fatigue Stress Range (MPa)
29	T+D	Weld toe	Flange	87.46
30	Crane	Weld toe	Flange	129.24

Table 21 Cross girder web attachment maximum fatigue stress range for ECA

6.2 Fatigue Estimates for Edge Girders (G1 and G4)

Fatigue estimates are presented below for weld defects at the toe and root in the edge girder splices. Results are presented in terms of number of days of the given cycles required until the initial defect (2mm height detection from NDT) grows to a critical size.

6.2.1 Flaws at Weld Toe (Type 1 flaws)

Fatigue estimates for vehicle loading scenarios based on existing flaws which are at the threshold detection depth for MPI primary inspection. Note that flaws have not been identified at the toe locations of splice welds in current inspections.

Fatigue ECA Case	Vehicle	Taper/Splice position	Weld Pre/Post Repair Grinding	Fatigue Stress Cycles considered (per day)	No Cycles to grow flaw to critical dimension (Days)		
					Initial Flaw 2x85mm	Initial Flaw 2x25mm	Initial Flaw 2x10mm
1a	1G	Upper	Pre	180 x 1G	93	159	303
2a	T+D	Upper	Pre	180 x T+D	86	147	281
3a	Crane	Upper	Pre	180 x Crane	17	34	81
4a	1G	Lower	Pre	180x1G	69	132	304
5a	T+D	Lower	Pre	180xT+D	63	120	281
6a	Crane	Lower	Pre	180xCrane	4	18	71
7a	1G	Upper	Post	180x1G	135	210	390
8a	T+D	Upper	Post	180xT+D	100	200	370
9a	Crane	Upper	Post	180xCrane	30	50	110
10a	1G	Lower	Post	180x1G	50	110	270
11a	T+D	Lower	Post	180xT+D	50	100	250
12a	Crane	Lower	Post	180xCrane	0	10	60

Table 22 Edge girder fatigue estimates for bottom flange splice weld toe defects.

6.2.2 Flaws at Weld Root, pre-grinding (Type 2a flaws)

The ECAs presented in 5.7.2 show that before flaws propagated from the weld root are removed, the through thickness defects from the root to weld surface have short critical lengths.

Fatigue estimates are provided for defects with surface length 3mm, 4mm and 5mm to indicate the rate of crack growth. However, the critical defects are sufficiently small that it is recommended that any visible root defects at the surface of the bottom flange splice welds are removed by grinding, as priority 1 defects were addressed.

In Table 23, no. cycle indicates the number of vehicles, of the type indicated that can pass over the bridge before the indicated starting defect size grows to a critical size. Note that MPI or PT inspection typically has a length sizing error of +-5mm which is incorporated in the defect sizes in the table.

ECA case	Vehicle	Taper/Splice position	No. cycles to critical from 3mm long defect	No. cycles to critical from 4mm long defect	No. cycles to critical from 5mm long defect
1b	1G	Upper	3866000	1205000	Defect critical
2b	T+D	Upper	3420000	1050000	Defect critical
3b	Crane	Upper	470000	90000	Defect critical
4b	1G	Lower	Defect critical	Defect critical	Defect critical
5b	T+D	Lower	Defect critical	Defect critical	Defect critical
6b	Crane	Lower	Defect critical	Defect critical	Defect critical

Table 23 No of cycles required to grow type 2a through thickness root defect to critical length for edge girders.

6.2.3 Flaws at Weld Root, post-grinding (Type 2b flaws)

The Type 2b flaws, residual root defect after grinding out high-risk weld defects, are difficult to detect and the critical height of the residual defect is small.

In terms of NDT inspection, measurement of the exposed root is similar to measuring the length of a surface defect. It is recommended that after grinding, the exposed weld face is finished to fine surface finish, i.e. polished, as this improves the detection capabilities of MPI inspection. The tables below show fatigue estimates for starting flaws of 1mm depth and 2mm depth, it is recommended to ensure that the surface finish and NDT system can identify flaws of this height.

ECA case	Vehicle	Taper/Splice position	Aspect Ratio a/2c (0.005)		Aspect Ratio a/2c (0.1)	
			Cycles to critical (1mm initial height)	Cycles to critical (2mm initial height)	Cycles to critical (1mm initial height)	Cycles to critical (2mm initial height)
7b	1G	Upper	6120000	450000	19410000	3660000
8b	T+D	Upper	5857000	337000	17243000	3251000
9b	Crane	Upper	894000	62000	2825000	544000
10b	1G	Lower	35000	0	97540	9170
11b	T+D	Lower	32400	0	89800	7300
12b	Crane	Lower	6400	0	20800	0

Table 24 Critical flaw heights at exposed weld face post-grinding for type 2b defects in edge girder bottom flange splice welds.

6.3 Fatigue Estimates for Internal Girders (G2 and G3)

Fatigue estimates are presented below for weld defects at the toe and root in the internal centre girder splices. Results are presented in terms of number of days of the given cycles required until the initial defect (2mm height detection from NDT) grows to a critical size.

6.3.1 Flaws at Weld Toe (Type 1 flaws)

Fatigue estimates for vehicle loading scenarios based on existing flaws which are at the threshold detection depth for MPI primary inspection. Note that flaws have not been identified at the toe locations of splice welds in current inspections.

Fatigue ECA Case	Vehicle	Taper/Splice position	Weld Pre/Post Repair Grinding	Fatigue Stress Cycles considered (per day)	No Cycles to grow flaw to critical dimension (Days)		
					Initial Flaw 2x85mm	Initial Flaw 2x25mm	Initial Flaw 2x10mm
13a	1G	Upper	Pre	180x1G	610	980	1630
14a	T+D	Upper	Pre	180xT+D	760	1220	2030
15a	Crane	Upper	Pre	180xCrane	170	280	505
16a	1G	Lower	Pre	180x1G	490	830	1560
17a	T+D	Lower	Pre	180xT+D	493	833	1573
18a	Crane	Lower	Pre	180xCrane	99	181	1680
19a	1G	Upper	Post	180x1G	650	1040	392
20a	T+D	Upper	Post	180xT+D	840	1360	1680
21a	Crane	Upper	Post	180xCrane	190	310	2200

Fatigue ECA Case	Vehicle	Taper/Splice position	Weld Pre/Post Repair Grinding	Fatigue Stress Cycles considered (per day)	No Cycles to grow flaw to critical dimension (Days)		
					Initial Flaw 2x85mm	Initial Flaw 2x25mm	Initial Flaw 2x10mm
22a	1G	Lower	Post	180x1G	330	580	550
23a	T+D	Lower	Post	180xT+D	330	580	1130
24a	Crane	Lower	Post	180xCrane	60	110	270

Table 25 Edge girder fatigue estimates for bottom flange splice weld toe defects.

6.3.2 Flaws at Weld Root, pre-grinding (Type 2a flaws)

The ECAs presented in 5.7.2 show that before flaws propagated from the weld root are removed, the through thickness defects from the root to weld surface have short critical lengths.

Fatigue estimates are provided for defects with surface length 3mm, 4mm and 5mm to indicate the rate of crack growth. However, the critical defects are sufficiently small that it is recommended that any visible root defects at the surface of the bottom flange splice welds are removed by grinding, as priority 1 defects were addressed.

In Table 26, no. cycle indicates the number of vehicles, of the type indicated that can pass over the bridge before the indicated starting defect size grows to a critical size. Note that MPI or PT inspection typically has a length sizing error of +-5mm which is incorporated in the defect sizes in the table.

ECA case	Vehicle	Taper/Splice position	No. cycles to critical from 3mm long defect	No. cycles to critical from 4mm long defect	No. cycles to critical from 5mm long defect
13b	1G	Upper	Not damaging	Not damaging	Defect critical
14b	T+D	Upper	Not damaging	Not damaging	Defect critical
15b	Crane	Upper	9206000	3202000	Defect critical
16b	1G	Lower	Defect critical	Defect critical	Defect critical
17b	T+D	Lower	Defect critical	Defect critical	Defect critical
18b	Crane	Lower	Defect critical	Defect critical	Defect critical

Table 26 No of cycles required to grow type 2a through thickness root defect to critical length for internal girder.

6.3.3 Flaws at Weld Root, post-grinding (Type 2b flaws)

The Type 2b flaws, residual root defect after grinding out high-risk weld defects, are difficult to detect and the critical height of the residual defect is small.

In terms of NDT inspection, measurement of the exposed root is similar to measuring the length of a surface defect. It is recommended that after grinding,

the exposed weld face is finished to fine surface finish, i.e. polished, as this improves the detection capabilities of MPI inspection. The tables below show fatigue estimates for starting flaws of 1mm depth and 2mm depth, it is recommended to ensure that the surface finish and NDT system can identify flaws of this height.

ECA case	Vehicle	Taper/Splice position	Aspect Ratio a/2c (0.005)		Aspect Ratio a/2c (0.1)	
			Cycles to critical (1mm initial height)	Cycles to critical (2mm initial height)	Cycles to critical (1mm initial height)	Cycles to critical (2mm initial height)
19b	1G	Upper	Not damaging	5110000	Not damaging	Not damaging
20b	T+D	Upper	Not damaging	6500000	Not damaging	Not damaging
21b	Crane	Upper	11430000	690000	Not damaging	6400000
22b	1G	Lower	170000	1750	460700	1030000
23b	T+D	Lower	177000	2000	468000	105000
24b	Crane	Lower	42000	0	116000	12000

Table 27 Critical flaw heights at exposed weld face post-grinding for type 2b defects in internal girder bottom flange splice welds.

6.4 Fatigue Estimates for Cross Girder

Fatigue ECA case	Vehicle	Flaw position	Member Considered	Fatigue Stress Cycles considered (per day)	No Cycles to grow flaw to critical dimension (Days)		
					Initial Flaw 2x85mm	Initial Flaw 2x25mm	Initial Flaw 2x10mm
25	1G	Weld toe	Web	180x1G	1507	2650	3549
26	T+D	Weld toe	Web	180xT+D	1397	2460	3297
27	Crane	Weld toe	Web	180xCrane	416	751	1025
28	1G	Weld toe	Flange	180x1G	0	71	359
28b	1G	Weld toe	Flange	180x1G (50% load)	888	1597	3997
29	T+D	Weld toe	Flange	180xT+D	0	55	322

Fatigue ECA case	Vehicle	Flaw position	Member Considered	Fatigue Stress Cycles considered (per day)	No Cycles to grow flaw to critical dimension (Days)		
					Initial Flaw 2x85mm	Initial Flaw 2x25mm	Initial Flaw 2x10mm
30	Crane	Weld toe	Flange	180xCrane	0	0	28

Table 28 Fatigue stress ranges for flaws at weld toes of stiffener attachments to cross girder.

6.5 Summary

The fatigue estimates presented how that many of assessment scenarios have short fatigue lives until the flaws detectable by NDT reach critical dimensions.

The governing findings for the girders are:

- Visible flaws at the surface of the weld throat extending from the root are likely to be critical at detectable length on the short ends of the bottom flange lower splices for all girders (G1 to G4) therefore they are recommended to be removed immediately. For the long ends of the upper splices, providing defects longer than 5mm are not present an inspection interval of 1 year is acceptable.

For residual defects at the exposed root of ground splice welds, the defects are sensitive to the capability of NDT detection:

- For the edge girder welds crane running is not recommended. Detection of 1mm height residual defects is required If 1mm flaw height can be detected, 6month inspection interval is acceptable.
- For the internal girder welds, crane running requires detection of 1mm height residual defect. If 1mm flaw height can be detected, 6month6 month inspection interval is acceptable.

Cranes should not be run in the outer lanes.

For potential defects at the weld toes of the splice welds 250 days between MPI inspection finding no defects larger than 2mm depth by 10mm length is acceptable.

A 2.5 year inspection interval is acceptable for welds to the cross girder webs. For welds to the cross girder flanges in the worst case position, inspection is recommended every 6 months, or every 5000 crane load cycles, whichever is shortest.

The fatigue estimates calculated here are used to inform the bridge management strategy discussed in Section 8.4.

7 Evaluation of risk of bridge collapse.

7.1 Outline

The load rating assessment model of the bridge has been utilised to investigate the possible behaviour of the bridge in the event of fracture of a girder at a welded girder splice whilst the bridge is loaded. This is an estimate of the behaviour of the bridge based on a static analysis utilising the bridge design code AS 5100 and the TMR Tier 1 Bridge Heavy Load Assessment Criteria (TMR BHLAC) methodology for calculating Strength Assessment Ratio (SAR) values.

The bridge is able to transfer loading to adjacent girders via the deck slab and the transverse cross girders as shown in Figure 37.

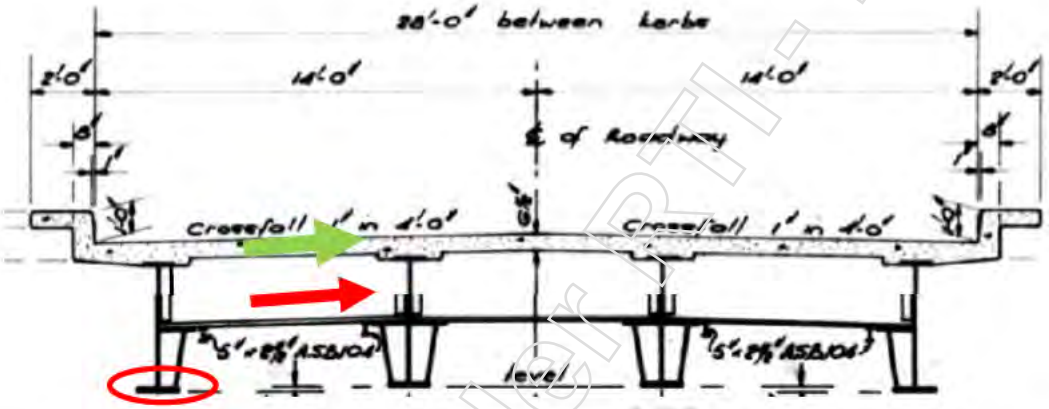

Figure 37: Example load distribution through internal girders and deck slab from edge girder fracture.

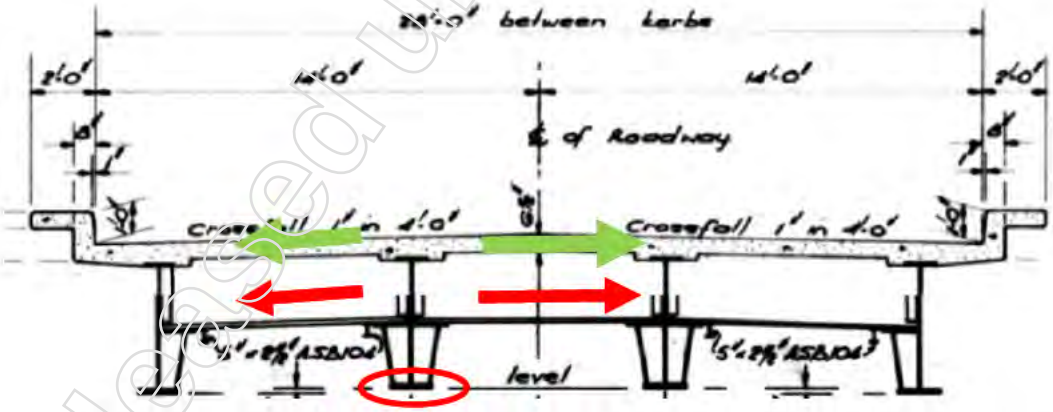

Figure 38: Example load distribution through cross girders and deck slab from middle girder fracture.

Should a tension flange undergo a brittle failure the effects on the bridge are assumed to be local loss of bending capacity in the steel composite girder.

The effects of fracture have been checked at twelve locations across the bridge on both an edge and internal girder. These locations are representative of all 72 splice locations (18 locations x 4 girders) across the bridge. Load effects in the main beams, cross girders and deck slab were obtained.

The models run are highlighted below and throughout the remainder of this section the assumed fracture location matches the relevant splice naming in the inspection report. Equivalent splices in spans 4, 5 and 6 are noted.

Splice id (spans 1 to 3)	Location	Equivalent Spans 4 – 6 id
S1 Spl1	Splice closest to abutments	S6 Spl3
S1 Spl2	Splice towards midspan	S6 Spl2
S1 Spl3	Splice in spans span 1 adjacent to haunch section to pier 1.	S6 Spl1
S2 Spl 1	In suspended span closest to abutments	S5 Spl2
S2 Spl 2	In suspended span closest to middle of bridge	S5 Spl1
S3 Spl 1	1 of 2 splices closest to pier 2. Also Similar to S1 Spl 3	S4 Spl4
S3 Spl 2	2 of 2 splices closest to pier 2	S4 Spl3
S3 Spl 3	Splice towards midspan	S4 Spl2
S3 Spl 4	Splice adjacent start pier 3 haunch. Similar to S1 Spl 3	S4 Spl1

Table 29 Summary of splice fracture locations checked.

Should a brittle fracture occur the bearings and joints in the bridge will be expected to articulate to allow for a partial collapse of the bridge superstructure. This is shown in the images below.

The assumed location of the girder fracture is shown approximately in red.

Location failure	Assumed post collapse form of the bridge.
Span 1 / Span 6 Span 2 acts as a structural fuse for a failure in span 1. Span 5 / 6 would behave in the same manner.	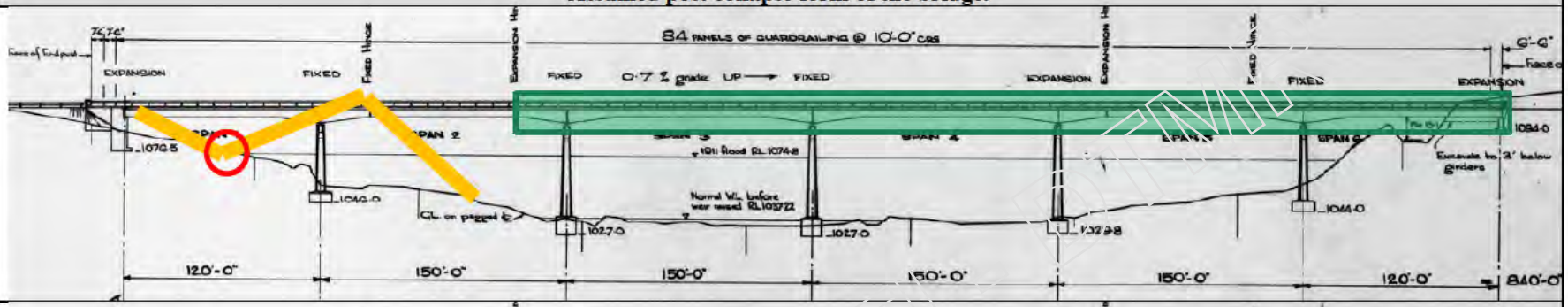
Span 2 / Span 5 Span 2 would collapse as a single section since it is supported on half joints	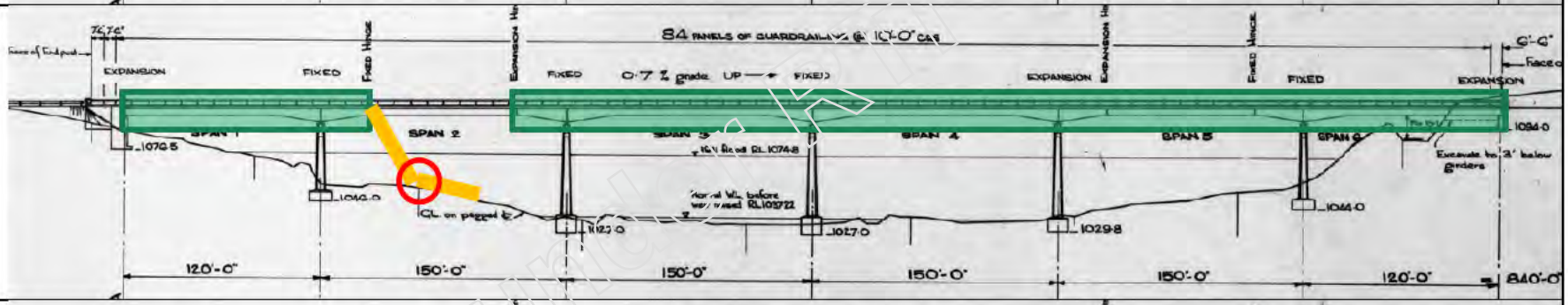
Span 3 / Span 4 The structure is continuous over pier 3 which allows for an amount of load redistribution within a girder. The suspended spans act as structural fuses.	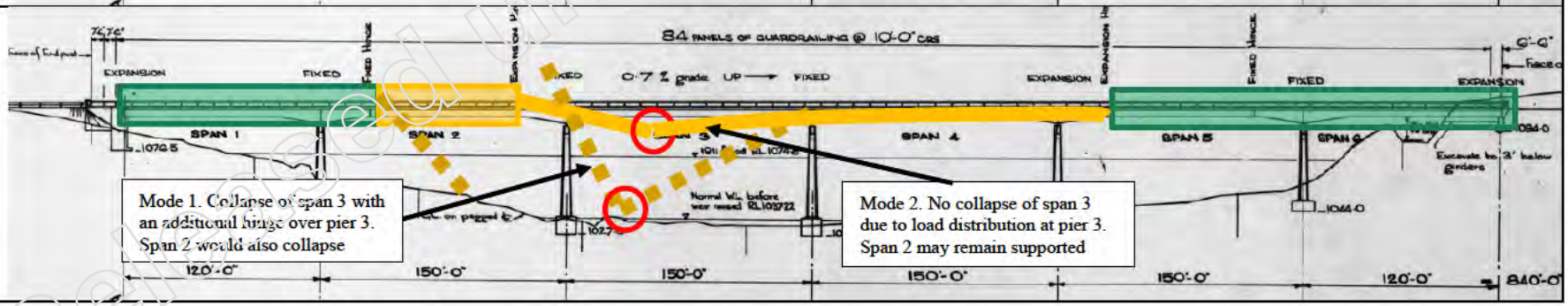

Table 30 Summary of splice fracture locations checked. Green is section of bridge expected to remain standing.

7.2 Modelling methodology

For the previous load rating work a 3d grillage model of the whole bridge was prepared. This is discussed in detail in the load rating report ref 267958/Rep001.

To evaluate the redistribution of loading caused by a failed flange, a moment hinge release was added in the bridge at the failure location. This is considered a reasonable assumption since the longitudinal load capacity of the deck slab only would be less than 1% of the composite girder. The dynamic effects of a brittle fracture are beyond the scope of this assessment.

At the fracture location the effects of the external post tensioning bending moment are applied as external loads to represent the beneficial load effects which are transferred across the hinge. Since the assumed hinge can transfer axial loads there is no requirement to revise the compression loading.

An example of the model is shown in Figure 39.

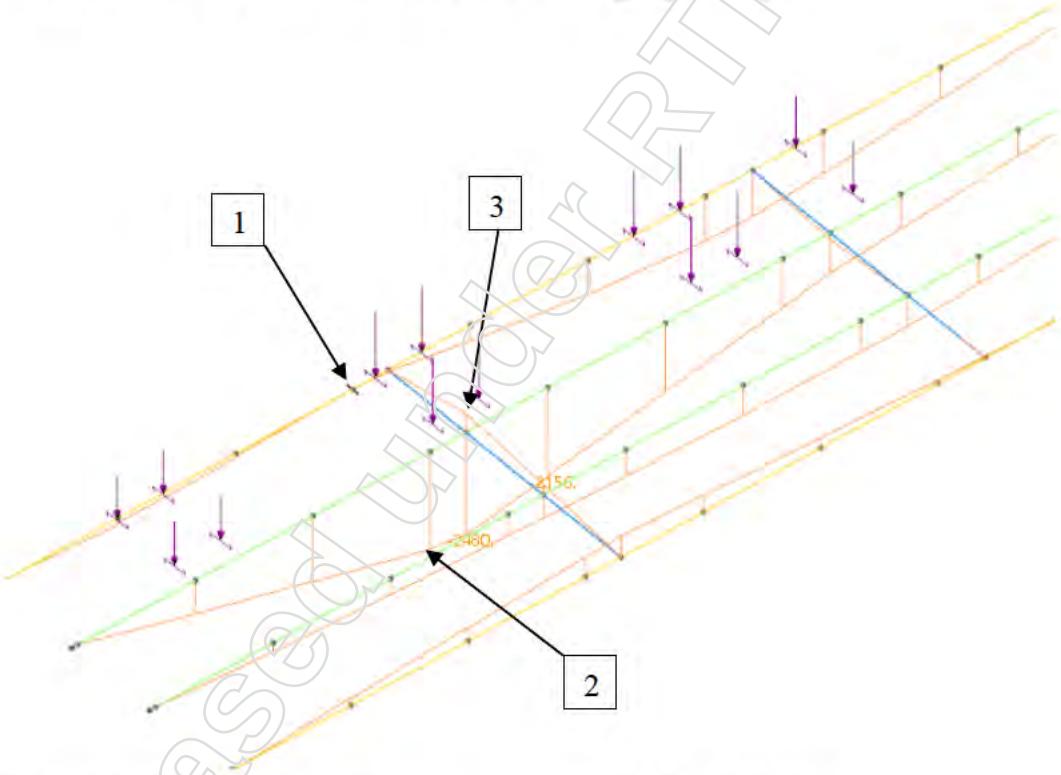

Figure 39: GSA model bending moment results with edge girder fracture

The following can be noted in the model

1. Zero bending moment at the hinge / fracture location in the edge girder as highlighted.
2. Significant additional bending moment in the adjacent internal girder
3. Significant bending moment in the transverse cross girders showing the load being distributed transversely between girders.

The deck slab is not shown but a similar increase in transverse load effects is observed.

Should a fracture occur in a flange it is assumed that the PT bars remain in service since these are anchored remote to all the splice locations. Longitudinal distribution in the concrete deck slab is not considered.

7.3 Vehicle loading

The following vehicles were adopted for the analysis.

- 42.5 t 1G semi trailer. DLA 0.4 and 0.1 (Veh 1G)
- 50.5 t Truck and Dog. DLA 0.4 and 0.1 (Veh 13 TnD)
- 79 t Crane. DLA 0.3 and 0.1 (Veh 4 79tCrn)

Note that the 48 t crane defined in the TMR BHLAC was also checked in the analysis model with the key load effects found to be similar to the 79 t crane due to its shorter length. The results for the 48 t crane are not reported.

The vehicles were placed in two lane, single lane and centreline running configurations as follows based on the TMR BHLAC.

- Restriction 1. Two lane running with vehicles placed adjacent to kerb or in marked lanes to obtain peak loading. Trailing vehicles are permitted.
- Restriction 3, Single lane running adjacent to kerb, marked lanes or along bridge centreline to obtain peak loading. No trailing vehicles.
- Restriction 5, Single lane running along bridge centreline to obtain peak loading. No trailing vehicles.
- Restriction 5T, Single lane running along bridge centreline to obtain peak loading. Trailing vehicles are permitted. This restriction is to investigate the effects of single lane running with a stream of vehicles along the bridge centreline.

Accompanying vehicles are assumed to be the same vehicle for the MCV cases and a Truck and Dog for the crane load case.

7.4 Results

For the assessment results below ULS load factors are applied. The dynamic load allowance (DLA) factors are assumed to be 0.4 and 0.1 to examine the expected effects of vehicle speeds on the bridge.

Should a fracture occur in a flange it is assumed that the PT bars remain in service since these are anchored remote to all the splice locations. Longitudinal distribution in the concrete deck slab is not considered.

With each of the failed girder models SAR values were calculated for the following elements to investigate the ability to redistribute the bridge loads.

- Main girders with redistributed DL and LL load effects.
- Transverse UB cross girders

- Transverse deck slab loading

Where the SAR number exceeds 1.0 there is a calculated reserve of capacity. Where the number is less than one this indicates that total dead and live loading applied loads exceed the calculated strength of the bridge.

7.4.1 Main girders

The table below summarises the SAR ratio of the bridge if a fracture occurs at a splice on the edge or internal girder. Only one fracture is assumed to occur. ULS load factors and material strength reduction factors are based on design values stated in AS 5100.

The SAR value stated is the minimum value for all elements in the main girders for all shear and moment load effects considered. The location stated is the fracture location and not the location of the minimum SAR value. The results for the column 'None' are those for an undamaged structure.

		Fracture location edge girder						
full DLA	Rest	None	S1 Spl 1	S1 Spl 2	S1 Spl 3	S2 Spl 1	S3 Spl 2	S3 Spl 3
Veh 13 TnD	1	1.07	0.69	0.90	0.73	0.83	0.85	1.07
Veh 13 TnD	3	1.26	0.88	1.25	1.06	1.02	1.12	1.26
Veh 13 TnD	5T	1.41	1.02	1.41	1.10	1.17	1.19	1.41
Veh 13 TnD	5	1.46	1.02	1.46	1.22	1.19	1.26	1.47
Veh 1G	1	1.04	0.67	0.93	0.72	0.80	0.87	1.04
Veh 1G	3	1.31	0.89	1.32	1.07	0.99	1.15	1.31
Veh 1G	5T	1.36	0.92	1.37	1.05	1.13	1.16	1.39
Veh 1G	5	1.51	1.03	1.51	1.23	1.16	1.30	1.52
Veh 4 79tCrn	1	0.97	0.63	0.76	0.66	0.74	0.74	0.97
Veh 4 79tCrn	3	1.08	0.76	0.99	0.90	0.87	0.92	1.08
Veh 4 79tCrn	5T	1.26	0.89	1.16	0.96	1.01	1.01	1.26
Veh 4 79tCrn	5	1.30	0.89	1.16	1.03	1.03	1.06	1.30

Table 31 Edge girder fracture. Summary of SAR values for main girders. DLA = 0.3 / 0.4

		Fracture location edge girder						
0.1 DLA	Rest	None	S1 Spl 1	S1 Spl 2	S1 Spl 3	S2 Spl 1	S3 Spl 2	S3 Spl 3
Veh 13 TnD	1	1.24	0.82	1.12	0.90	0.97	1.02	1.24
Veh 13 TnD	3	1.44	1.03	1.44	1.29	1.18	1.30	1.44
Veh 13 TnD	5T	1.57	1.17	1.58	1.34	1.34	1.38	1.58
Veh 13 TnD	5	1.62	1.18	1.63	1.47	1.36	1.45	1.63
Veh 1G	1	1.21	0.79	1.16	0.89	0.95	1.03	1.21
Veh 1G	3	1.49	1.04	1.50	1.31	1.15	1.34	1.49
Veh 1G	5T	1.53	1.08	1.55	1.28	1.30	1.35	1.55
Veh 1G	5	1.68	1.19	1.68	1.49	1.33	1.49	1.68
Veh 4 79tCrn	1	1.09	0.72	0.90	0.78	0.84	0.85	1.09

		Fracture location edge girder						
0.1 DLA	Rest	None	S1 Spl 1	S1 Spl 2	S1 Spl 3	S2 Spl 1	S3 Spl 2	S3 Spl 3
Veh 4 79tCrn	3	1.20	0.86	1.15	1.03	0.98	1.04	1.20
Veh 4 79tCrn	5T	1.37	0.99	1.33	1.11	1.12	1.13	1.38
Veh 4 79tCrn	5	1.41	0.99	1.34	1.19	1.15	1.18	1.42

Table 32 Edge girder fracture. Summary of SAR values for main girders. DLA = 0.1

		Fracture location internal girder						
full DLA	Rest	None	S1 Spl 1	S1 Spl 2	S1 Spl 3	S2 Spl 1	S3 Spl 2	S3 Spl 3
Veh 13 TnD	1	1.07	1.03	1.17	0.90	1.06	1.03	1.07
Veh 13 TnD	3	1.26	1.26	1.45	1.24	1.26	1.26	1.26
Veh 13 TnD	5T	1.41	1.41	1.57	1.35	1.41	1.42	1.41
Veh 13 TnD	5	1.46	1.46	1.63	1.46	1.46	1.47	1.46
Veh 1G	1	1.04	0.99	1.15	0.88	1.02	1.04	1.04
Veh 1G	3	1.31	1.31	1.49	1.26	1.29	1.31	1.31
Veh 1G	5T	1.36	1.36	1.53	1.28	1.38	1.37	1.36
Veh 1G	5	1.51	1.51	1.66	1.50	1.52	1.52	1.51
Veh 4 79tCrn	1	0.97	0.93	1.02	0.81	0.97	0.87	0.97
Veh 4 79tCrn	3	1.08	1.08	1.20	1.05	1.08	1.06	1.08
Veh 4 79tCrn	5T	1.26	1.26	1.38	1.18	1.26	1.24	1.26
Veh 4 79tCrn	5	1.30	1.30	1.41	1.26	1.30	1.29	1.30

Table 33 Internal girder fracture. Summary of SAR values for main girders. DLA = 0.3 / 0.4

		Fracture location internal girder						
0.1 DLA	Rest	None	S1 Spl 1	S1 Spl 2	S1 Spl 3	S2 Spl 1	S3 Spl 2	S3 Spl 3
Veh 13 TnD	1	1.24	1.24	1.17	1.10	0.82	1.24	1.24
Veh 13 TnD	3	1.44	1.44	1.45	1.44	1.03	1.44	1.44
Veh 13 TnD	5T	1.57	1.58	1.57	1.58	1.17	1.58	1.58
Veh 13 TnD	5	1.62	1.63	1.63	1.63	1.18	1.63	1.63
Veh 1G	1	1.21	1.20	1.15	1.08	0.79	1.21	1.21
Veh 1G	3	1.49	1.49	1.49	1.47	1.04	1.49	1.49
Veh 1G	5T	1.53	1.53	1.53	1.53	1.08	1.54	1.53
Veh 1G	5	1.68	1.68	1.66	1.68	1.19	1.68	1.68
Veh 4 79tCrn	1	1.09	1.07	1.02	0.95	0.72	1.01	1.09
Veh 4 79tCrn	3	1.20	1.20	1.20	1.20	0.86	1.20	1.20
Veh 4 79tCrn	5T	1.37	1.37	1.38	1.36	0.99	1.38	1.38
Veh 4 79tCrn	5	1.41	1.41	1.41	1.41	0.99	1.42	1.41

Table 34 Internal girder fracture. Summary of SAR values for main girders. DLA = 0.1

From the above it can be seen that the edge girder fracture is more sensitive than the internal girder fracture and this is to be expected since the loads can only be distributed to one side towards the internal girders.

7.4.2 Cross girders

The ability of the cross girders to distribute load is governed by the strength of the TB/ TF connections which connect the cross girders to the main girders. As discussed previously the connecting plates are slotted through the main girders and the cross girders are fully continuous across the bridge.

Figure 40: Typical internal cross girder member and connection.

The cross girders comprise 762x267x197kg UB sections which are connected to the main girders with TF / TB bolts. A summary of the capacities is shown below and it can be seen that the connections govern the available strength of the cross girder assemblies. No composite action is available since no studs are provided in the cross girders.

- Cross Girder capacity 1289 kNm bending / 1490 kN shear
- Moment capacity girder 1 & 4. 366 kNm from 4 No. 7/8" (22mm) TB bolts
- Moment capacity girder 2 & 3 916 kNm from 10 No. 7/8" (22mm) TB bolts
- Shear capacity all girders downward direction. 1490 kN based on bearing of cross girder as shown above which allows full beam strength to be developed.
- Shear capacity all girders upwards direction 497 kN from 4 bolts in shear. 4 No. 7/8" (22mm) TB bolts.\

It is noted that the bolts on the bottom flange would also allow for additional capacity since they would also need to fail in tension. A reduction in bending

capacity would need to be considered. However the limiting SAR values for the cross girders is typically the bending capacity of the connection hence the upward shear capacity has not been enhanced.

The SAR value stated is the minimum value for all elements in the cross girders for all shear and moment load effects considered. The location stated is the fracture location and not the location of the minimum SAR value. The results for the column 'None' are those for an undamaged structure.

		Fracture location edge girder						
full DLA	Rest	Existing	S1 Spl 1	S1 Spl 2	S1 Spl 3	S2 Spl 1	S3 Spl 2	S3 Spl 3
Veh 13 TnD	1	3.11	0.43	1.12	0.74	0.41	1.58	1.05
Veh 13 TnD	3	3.47	0.55	1.62	1.13	0.50	2.00	1.62
Veh 13 TnD	5T	4.23	0.71	2.16	1.65	0.64	2.01	1.86
Veh 13 TnD	5	4.24	0.71	2.17	1.66	0.65	2.19	2.08
Veh 1G	1	1.04	0.67	0.93	0.72	0.80	0.87	1.04
Veh 1G	3	1.31	0.89	1.32	1.07	0.99	1.15	1.31
Veh 1G	5T	1.36	0.92	1.37	1.05	1.13	1.16	1.39
Veh 1G	5	1.51	1.03	1.51	1.23	1.16	1.30	1.52
Veh 4 79tCrn	1	3.63	0.41	1.06	0.68	0.38	1.48	1.03
Veh 4 79tCrn	3	3.63	0.47	1.26	0.85	0.43	1.75	1.29
Veh 4 79tCrn	5T	3.63	0.61	1.78	1.22	0.55	1.92	1.59
Veh 4 79tCrn	5	3.63	0.61	1.78	1.22	0.56	2.02	1.81

Table 35 Edge girder fracture. Summary of SAR values for cross girders. DLA = 0.3 / 0.4

		Fracture location edge girder						
0.1 DLA	Rest	Existing	S1 Spl 1	S1 Spl 2	S1 Spl 3	S2 Spl 1	S3 Spl 2	S3 Spl 3
Veh 13 TnD	1	3.73	0.50	1.33	0.92	0.48	1.81	1.20
Veh 13 TnD	3	4.13	0.63	1.87	1.39	0.57	2.23	1.76
Veh 13 TnD	5T	5.34	0.79	2.42	1.97	0.71	2.42	1.98
Veh 13 TnD	5	5.35	0.79	2.43	1.99	0.71	2.63	2.17
Veh 1G	1	3.99	0.47	1.40	0.91	0.47	1.78	1.26
Veh 1G	3	4.98	0.64	1.94	1.49	0.57	2.24	1.75
Veh 1G	5T	5.36	0.75	2.35	2.11	0.70	2.32	2.20
Veh 1G	5	5.59	0.82	2.47	2.12	0.71	2.77	2.29
Veh 4 79tCrn	1	4.07	0.46	1.21	0.79	0.43	1.64	1.14
Veh 4 79tCrn	3	4.71	0.52	1.42	0.98	0.47	1.91	1.40
Veh 4 79tCrn	5T	4.71	0.66	1.95	1.40	0.60	2.19	1.70
Veh 4 79tCrn	5	4.71	0.67	1.96	1.40	0.61	2.30	1.90

Table 36 Edge girder fracture. Summary of SAR values for cross girders. DLA = 0.1

		Fracture location internal girder						
full DLA	Rest	Existing	S1 Spl 1	S1 Spl 2	S1 Spl 3	S2 Spl 1	S3 Spl 2	S3 Spl 3
Veh 13 TnD	1	3.11	0.69	0.99	0.97	0.73	1.33	1.43
Veh 13 TnD	3	3.47	0.89	1.12	1.45	0.92	1.70	1.80
Veh 13 TnD	5T	4.23	0.87	1.17	1.42	0.92	1.79	1.60
Veh 13 TnD	5	4.24	0.89	1.17	1.55	0.92	1.85	1.80
Veh 1G	1	1.04	0.99	1.15	0.88	1.02	1.04	1.04
Veh 1G	3	1.31	1.31	1.49	1.26	1.29	1.31	1.31
Veh 1G	5T	1.36	1.36	1.53	1.28	1.38	1.37	1.36
Veh 1G	5	1.51	1.51	1.66	1.50	1.52	1.52	1.51
Veh 4 79tCrn	1	3.63	0.67	0.97	0.87	0.68	1.25	1.36
Veh 4 79tCrn	3	3.63	0.80	1.07	1.24	0.81	1.51	1.49
Veh 4 79tCrn	5T	3.63	0.79	1.14	1.25	0.79	1.63	1.36
Veh 4 79tCrn	5	3.63	0.80	1.14	1.34	0.81	1.68	1.49

Table 37 Internal girder fracture. Summary of SAR values for cross girders. DLA = 0.3 / 0.4

		Fracture location internal girder						
0.1 DLA	Rest	Existing	S1 Spl 1	S1 Spl 2	S1 Spl 3	S2 Spl 1	S3 Spl 2	S3 Spl 3
Veh 13 TnD	1	3.73	0.83	0.99	1.19	0.50	1.50	1.73
Veh 13 TnD	3	4.13	1.06	1.12	1.75	0.63	1.87	2.12
Veh 13 TnD	5T	5.34	1.04	1.17	1.71	0.79	1.96	1.92
Veh 13 TnD	5	5.35	1.06	1.17	1.86	0.79	2.01	2.15
Veh 1G	1	3.99	0.81	1.01	1.18	0.47	1.54	1.70
Veh 1G	3	4.98	1.04	1.11	1.78	0.64	1.91	2.03
Veh 1G	5T	5.36	0.96	1.14	1.64	0.75	1.95	1.96
Veh 1G	5	5.59	1.04	1.14	1.89	0.82	2.05	2.04
Veh 4 79tCrn	1	4.07	0.78	0.97	1.03	0.46	1.38	1.56
Veh 4 79tCrn	3	4.71	0.90	1.07	1.42	0.52	1.63	1.69
Veh 4 79tCrn	5T	4.71	0.90	1.14	1.44	0.66	1.75	1.56
Veh 4 79tCrn	5	4.71	0.90	1.14	1.53	0.67	1.80	1.69

Table 38 Internal girder fracture. Summary of SAR values for cross girders. DLA = 0.1

It can be seen that the cross girders adjacent to splice SP1 and SP4 are subject to the largest load effects. This is because a cross girder is provided in close proximity to the fractured splice.

7.4.3 Deck slab results

Transverse distribution of loads between adjacent girders can also be achieved through the deck slab, besides the cross girders. The figure below shows the assumed yield lines in the slab for a fracture of the edge girder.

The record drawings show that the cross girders are not composite with the deck slab hence the distribution from the cross girders and slab can be considered independently.

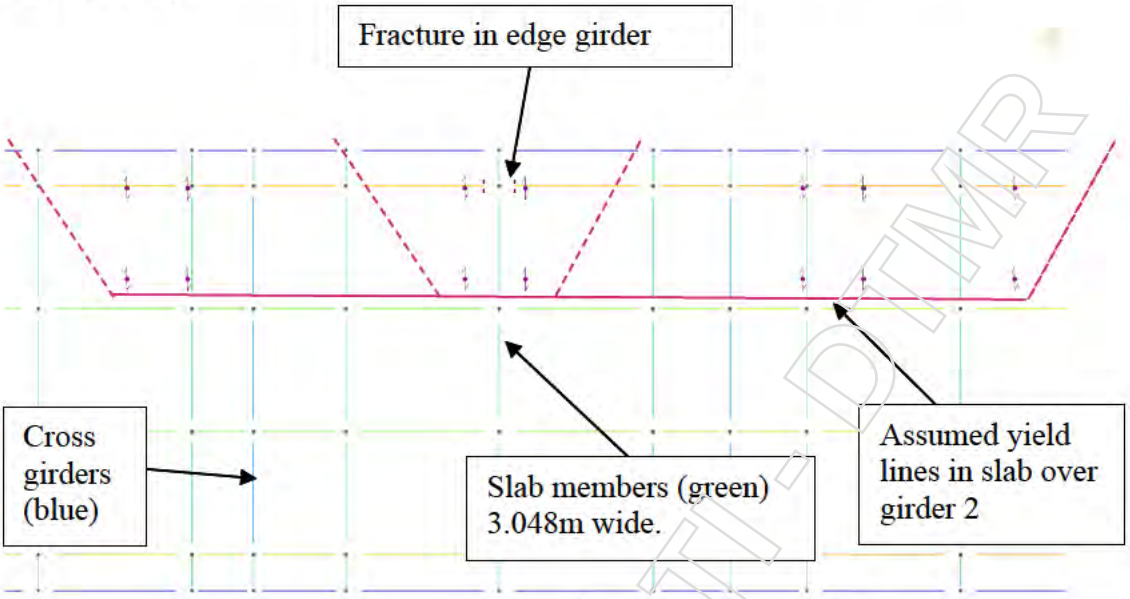

Figure 41: Slab load distribution assumptions. (Truck and Dog shown)

Based on the as-built drawings bending capacities of the slab have been estimated from the main grillage model. The deck slab comprises 6 ½ " thick slab with 20 MPa concrete assumed and 230 MPa reinforcement. Bent up bars were provided in the original design to reduce the amount of reinforcement.

∅Mu hog over girders = 35.9 kNm/m width

∅Mu sag over girders = -21.6 kNm/m width

Within the GSA assessment model the continuous deck slab is represented as 3.048m wide strips of deck over the length of the bridge. The slab elements close to the fracture location are subject to large bending moments however for bending failure to occur the slab must yield over a longer length up to the length of the vehicle. Thus SAR values have been calculated as follows.

- SAR value for single 3m wide slab element with peak loads at fracture location from DL + LL effects
- SAR value for single 3m wide slab element with peak loads at fracture location from DL only. This is to check the contribution of the live loading.
- SAR value for 3m wide slab element + adjacent 3m slab elements which represents a 9m section of bridge slab. The coexisting effects are combined and checked against the capacity of the 9m section. This smooths the peak effect adjacent to the fracture location.

Finally the length of slab along the yield line that is required to support the combined loads from the 9m section is calculated (provide a SAR = 1). The aim of the slab length calculation is to provide an estimate on if the length of slab required is more than the length of the vehicle causing the applied loading. The vehicles are assumed to have the following lengths between front and rear axles.

- Truck and Dog 50.5t. 17.6m overall

The calculations are carried out for yield lines forming over the edge girder 1, and internal girders 2 & 3 with the worst case reported.

	Veh 13. TnD left lane. SAR Values						
	Fracture location in Edge Girder	S1 Spl1	S1 Spl2	S1 Spl3	S2 Spl1	S3 Spl 2	S3 Spl 3
Girder 1	SAR 3m section	0.27	0.29	0.54	2.31	0.24	0.85
	SAR 3m section DL	0.91	3.45	9.58	4.21	0.69	2.86
	SAR 9m section	0.99	0.94	1.79	2.68	0.79	3.28
	length (m)	9.2	9.7	5.1	3.4	11.6	2.8
Girder 2 3	SAR 3m section	0.30	0.26	0.37	1.69	0.22	0.80
	SAR 3m section DL	0.91	1.55	17.22	4.91	0.58	1.93
	SAR 9m section	0.85	0.53	0.97	2.01	0.57	1.86
	length (m)	10.8	17.3	9.4	4.6	16.2	4.9
	Veh 13. TnD on bridge centreline. SAR Values						
	Fracture location in Edge Girder	S1 Spl1	S1 Spl2	S1 Spl3	S2 Spl1	S3 Spl 2	S3 Spl 3
Girder 1	SAR 3m section	0.44	0.61	1.35	2.84	0.38	1.62
	SAR 3m section DL	0.91	3.45	9.58	4.21	0.69	2.86
	SAR 9m section	1.96	2.32	2.72	3.19	1.44	5.51
	length (m)	4.7	3.9	3.4	2.9	6.4	1.7
Girder 2 3	SAR 3m section	0.51	0.51	0.74	3.89	0.36	1.49
	SAR 3m section DL	0.91	1.55	17.22	4.91	0.58	1.93
	SAR 9m section	1.47	1.13	1.93	4.72	0.96	3.53
	length (m)	6.2	8.1	4.7	1.9	9.5	2.6

Table 39 Truck & Dog, summary of deck slab SAR results for edge girder fracture.

	Veh 13. TnD left lane. SAR Values						
	Fracture location in Internal Girder	S1 Spl1	S1 Spl2	S1 Spl3	S2 Spl1	S3 Spl 2	S3 Spl 3
Girder 1	SAR 3m section	1.32	1.05	2.23	8.81	0.76	2.36
	SAR 3m section DL	2.77	2.97	9.87	9.06	1.34	3.56
	SAR 9m section	3.01	2.39	3.39	9.19	1.91	4.01
	length (m)	3.0	3.8	2.7	1.0	4.8	2.3
Girder 2 3	SAR 3m section	0.41	0.24	0.66	9.21	0.18	0.74
	SAR 3m section DL	1.07	1.31	15.80	34.76	0.38	1.57
	SAR 9m section	1.38	0.50	1.82	9.53	0.47	2.07
	length (m)	6.6	18.4	5.0	1.0	19.5	4.4
	Veh 13. TnD on bridge centreline. SAR Values .						
	Fracture location in Internal Girder	S1 Spl1	S1 Spl2	S1 Spl3	S2 Spl1	S3 Spl 2	S3 Spl 3
Girder	SAR 3m section	1.38	1.08	2.16	7.36	0.77	2.16
	SAR 3m section DL	2.77	2.97	9.87	9.06	1.34	3.56

	SAR 9m section	3.23	2.59	3.69	7.65	2.01	4.18
	length (m)	2.8	3.5	2.5	1.2	4.6	2.2
Girder 2 3	SAR 3m section	0.42	0.26	0.69	4.98	0.19	0.69
	SAR 3m section DL	1.07	1.31	15.80	34.76	0.38	1.57
	SAR 9m section	1.19	0.51	1.50	5.23	0.49	1.50
	length (m)	7.7	17.9	6.1	1.7	18.8	6.1

Table 40 Truck & Dog, summary of deck slab SAR results for internal girder fracture.

7.5 Summary

7.5.1 Selected results

The table below summarise critical results from the tables above for the 50.5 t Truck and Dog vehicle. It is noted that the load effects from the 42.5 t Semi Trailer are similar due to the shorter length of the vehicle which can allow for additional loads from a trailing vehicle.

The selected locations show the distribution provided by the cross girders and the deck slab. S1 Spl1 is situated in proximity to a cross girder and S1 Spl 2 is further from the cross girder with greater distribution from the deck slab.

Vehicle and location	Edge girder location of fractured splice plate	SAR Values		
		Main beams	Cross girders	Slab
Veh 13 TnD in both lanes together (Restriction 1)	S1 Spl 1	0.69	0.43	0.85
	S1 Spl 2	0.90	1.12	0.53
Veh 13 TnD single vehicle in marked lane (Restriction 3)	S1 Spl 1	0.88	0.55	>0.85
	S1 Spl 2	1.25	1.62	>0.53
Veh 13 TnD single vehicle on bridge centreline (Restriction 5)	S1 Spl 1	1.02	0.71	1.47
	S1 Spl 2	1.46	2.17	1.13

Table 41 Truck & Dog, summary of SAR results for internal girder fracture.

Vehicle and location	Internal girder location of fractured splice plate	SAR Values		
		Main beams	Cross girders	Slab
Veh 13 TnD in both lanes together (Restriction 1)	S1 Spl 1	0.90	0.69	1.38
	S1 Spl 2	0.99	0.99	0.50
Veh 13 TnD single vehicle in marked lane (Restriction 3)	S1 Spl 1	1.24	0.89	>1.38
	S1 Spl 2	1.45	1.12	>0.50
Veh 13 TnD single vehicle on bridge centreline (Restriction 5)	S1 Spl 1	1.46	0.89	1.19
	S1 Spl 2	1.63	1.17	0.51*

Table 42 Truck & Dog, summary of SAR results for edge girder fracture. * See section 7.5.4 below.

It can be seen from the results tables that where the SAR value for the cross girders improve then the SAR values for the deck slab decrease.

For the edge girder fracture case it can be seen that no SAR values exceed 1 for restriction 1. As the vehicles are limited in number and location (restrictions 3 and 5) then typically the SAR for either slab or cross girder does exceed 1.

For the internal girder fracture the results are improved which is to be expected due to the improved load distribution. The S1 Spl 2 slab SAR value of 0.51 is low and this is discussed in section 7.5.4 below.

7.5.2 Main girder

It can be seen in the results tables that the amount of overstress is more limited should a fracture occur in an internal rather than an edge girder. This is expected since the fractured girder is able to redistribute loads to two adjacent girders rather than one.

Based on Table 30 a fracture in span 1 (or span 6) has potential to cause two spans to collapse compared to less should a fracture occur in spans 3 to span 6.

7.5.3 Cross girders

From the results tables it is noted that fractures occurring at splices S1 Spl1 and S2 Spl1 cause significant loads in the cross-girder members. This is because the cross girders at this location are very close to the splice detail thus attracting significant loads. As shown by the SAR values, the load effects for a fracture in the edge girder are worse than those for a fracture of the internal girders.

As noted above the cross girder capacity is governed by the moment connection through the main girder / thus additional capacity could be gained with additional bolting.

7.5.4 Deck slab

From the results tables it is noted that a fracture at splice S3 Spl 2 shows the most significant loads in the deck slab, This is caused by the applied loads and placement of the cross girder which is not directly at the splice. Splice S1 Spl1 also shows a similar effect.

It is noted that similar SAR values arise for both the internal and external girder fractures. This is due to the bent up bar reinforcement detailing which varies the hogging and sagging capacity of the deck slab over the girders.

For the edge girder fracture cases, high transverse hogging moments are generated over the adjacent internal girder however the bending capacity is also greater.

For the internal girder fracture cases, transverse sagging moments are generated over the fracture location and the load is distributed in two directions. However the sagging capacity over the girder is less which leads to a similar SAR value to the edge girder case. The SAR value for the sagging over girder 2 is 0.51 and a review of the calculations indicates that the SAR value for the hogging over the adjacent internal girder is 1.96 indicating a substantial reserve available for

redistribution of the transverse moments. Hence the actual performance of the bridge for this load case is likely much better than the indicated SAR value.

7.5.5 Overall

From the above results it can be seen that for multiple elements are identified with overstress in the event of a brittle fracture of a main bridge girder. This is not unexpected. It is noted that the assessment is carried out for ULS applied loads and ULS capacities however the loading on the bridge at failure would be reasonably expected to be at an SLS level. This application of ULS loads is justified since a brittle failure of a bridge girder would be a highly dynamic structural situation.

For vehicle loads the ultimate load factor is 2.0 which would reduce to 1.0 for serviceability hence it would be expected that SAR values greater than 0.5 would approach a value of 1 depending on the amount of permanent load effects. It can be seen that several values for the cross girders and deck slab are less than 0.5 though for the internal fracture scenarios there is a reserve of strength in the slab.

It is noted that the fractures in the edge girder splices cause significantly more elements with SAR values less than 1 thus the edge girders should be a priority for inspection and any anticipated remedial works.

The assessment is not intended to justify continued operation of the bridge post fracture, only to examine the vehicle loading configuration which is likely to provide the maximum redundancy for the structure. It is not intended that the bridge would operate with a fractured girder. This assessment shows that the ability of the bridge to redistribute the vehicle loading in the event of a girder fracture is maximised with a reduced speed and vehicles positioned on the bridge centreline.

8 Bridge Management Strategy

The ECAs and fatigue estimates presented in Sections 5 and 6 are intended to be used to inform an NDT inspection strategy which can be used to manage the ongoing use of the bridge, controlling the risk of brittle failure.

The main recommendations from the calculations presented are that:

1. The outer running lanes be restricted to 1G and Truck and Dog vehicles only to limit the applied stresses to the edge girder steelwork. In the event of a brittle fracture it is noted that the calculations indicate multiple elements are overstressed.
2. Cranes and other heavy vehicles should not be run in the outer lanes. This is to limit the applied stresses in the edge girders
3. Crane vehicles may be run in the centre lane with additional consideration of stress levels. A 79t crane was assumed for this assessment. The 48 t crane defined in the TMR BHLAC was also checked and found cause similar bending effects to the 79 t crane. Any approvals for this type of loading should be based on the applied stresses rather than the length and weight of the vehicle.

Where the inspections identify a defect then allowable sizes are noted in the tables in section 5.7.1 to 5.7.4.

8.1 Interpretation of NDT/Inspection Flaws

Limiting flaw dimensions to control the risk of brittle fracture have been calculated for the G1 to G4 bottom flange splice welds and stiffener to cross girder welds. These are summarised in Section 5.

The NDT methodology to be used to monitor the structure is primarily MPI (Magnetic Particle Inspection) and PT (liquid Penetrant Testing) with UT (Ultrasonic Testing) available for further investigation of potential defects. This section of the report details how the results of an NDT survey can be used to assess the risk of identified flaws on the structure. The NDT system, i.e. technique, usage and environmental factors has been assumed to have reliability and detection capabilities as specified in Annex T of BS7910.

The critical flaw dimensions from the ECAs in Section 5.7 are summarised below.

Location	Weld Detail	Max. Vehicle	Critical Flaw Height/Depth, a (mm)	Critical Flaw Length, 2c (mm)
Edge girder (G1 and G4)	Flange Splice, toe defect	T+D	2.4	96
Internal girder (G2 and G3)	Flange Splice, toe defect	Crane	2.0	80
Edge Girder (G1 and G4)	Pre-grinding, exposed flaw at splice weld surface from root	T+D	Through thickness	5.6

Location	Weld Detail	Max. Vehicle	Critical Flaw Height/Depth, a (mm)	Critical Flaw Length, 2c (mm)
Internal Girder (G2 and G3)	Pre-grinding, exposed flaw at splice weld surface from root	Crane	Through thickness	6.0
Edge Girder (G1 and G4)	Post-grinding, exposed flaw at exposed root of splice weld	T+D	1.7mm	Full length of weld
Internal Girder (G2 and G3)	Post-grinding, exposed flaw at exposed root of splice weld	Crane	1.7mm	Full length of weld
Cross Girder	Toe defect, stiffener weld to cross girder web	Crane	4.7	190
Cross Girder	Toe defect, stiffener weld to cross girder flange	Crane	1.4	56

Table 43 Summary of critical flaw dimensions.

Cases highlighted in green in Table 43, are within the detection capabilities of surface MPI according to Annex T of BS7910, sizing error is accounted for in the calculations. It is recommended the NDT system employed on site is capable of the required detection. Cases highlighted in orange are likely to require enhanced NDT due to the size of flaw which must be detected. This may include surface finishing such as grinding or polishing or increasing the sensitivity of the NDT system.

If this cannot be achieved, then alternative solutions such as toe grinding to remove potential toe defects, weld repair or reducing vehicle load may be required.

8.2 Inspection Intervals

Location	Flaw Type	Detail	Inspection Interval	Requirements
Edge girder (G1 and G4)	1	Flange Splice Upper toe defect	9 months	No defect identified with MPI, no crane running outer lane.
Edge girder (G1 and G4)	1	Flange Splice Lower toe defect	8 months	No defect identified with MPI, no crane running outer lane.
Internal girder (G2 and G3)	1	Flange Splice Upper toe defect	16 months	No defect identified with MPI
Internal girder (G2 and G3)	1	Flange Splice Lower toe defect	9 months	No defect identified with MPI

Location	Flaw Type	Detail	Inspection Interval	Requirements
Edge Girder (G1 and G4)	2a	Pre-grinding, exposed flaw at splice weld surface from root, upper splices	1 year	4mm surface defect identified with MPI, no crane running
Edge Girder (G1 and G4)	2a	Pre-grinding, exposed flaw at splice weld surface from root, lower splices	Recommend grinding weld out	Grind weld until exposed root meets type 2b requirements
Internal Girder (G2 and G3)	2a	Pre-grinding, exposed flaw at splice weld surface from root, upper splices	1 year	4mm surface defect identified with MPI, no crane running
Internal Girder (G2 and G3)	2a	Pre-grinding, exposed flaw at splice weld surface from root, lower splices	Recommend grinding weld out	Grind weld until exposed root meets type 2b requirements
Edge Girder (G1 and G4)	2b	Post-grinding, exposed flaw at exposed root of splice weld, upper splices	3 years	Maximum height of exposed root defect 2mm. Suggest MPI or PT with surface treatment
Edge Girder (G1 and G4)	2b	Post-grinding, exposed flaw at exposed root of splice weld, lower splices	6 months	exposed root defect 1mm. Suggest MPI or PT with surface treatment
Internal Girder (G2 and G3)	2b	Post-grinding, exposed flaw at exposed root of splice weld, upper splices	3 years	Maximum height of exposed root defect 2mm. Suggest MPI or PT with surface treatment
Internal Girder (G1 to G2)	2b	Post-grinding, exposed flaw at exposed root of splice weld, lower splices	6 months	exposed root defect 1mm. Suggest MPI or PT with surface treatment
Cross Girder	-	Toe defect, stiffener weld to cross girder web	2.5 years	
Cross Girder	-	Toe defect, stiffener weld to cross girder flange	6 months / 5000 crane load cycles	No defect identified with MPI

Table 44 Inspection interval recommendations for critical weld details.

Note that the inspection regime can be fine-tuned such that details less susceptible to fatigue may be inspected less frequently.

Due to uncertainties in some properties used in the assessment, such as number of vehicles, fatigue crack growth material properties and flaw idealisation, the inspection intervals may be reviewed after a period of time if no flaw growth is observed.

Direct measurement of stresses in the bridge under vehicle loading may allow for a revised estimate of the fatigue crack growth and an increase in the inspection intervals for the bridge.

8.3 Methodology for Treating Flaws Identified During Inspection

Treatment of identified flaws is discussed for each flaw type.

8.3.1 Weld toe defects (Type 1 or cross girder)

Where weld toe defects are identified by NDT. The measure length should be checked against the relevant critical flaw height versus length chart in Section 5.7. This should provide indication, for typical flaw aspect ratios, whether the flaw depth may be critical. If the chart suggests that the flaw depth may not be critical, the inspection interval given in 8.2 should be followed.

If the critical flaw depth versus length chart suggests a critical flaw depth from the measure length is feasible, or the flaw has grown since the last inspection, the defect depth should be measure by UT or ACFM. (Alternating Current Field Measurement). If the measured defect depth is critical, the defect should be removed or repaired by toe grinding. Otherwise the inspection interval given in 8.2 should be followed.

8.3.2 Bottom Flange Splice, defects at surface of weld throat (Type 2a)

This defect type has been commonly found on splice connections on the structure and were previously categorised as priority 1 cracks. Multiple cracks were removed from the structure by grinding. For remaining flaws, the critical length is small as reported in Section 5.7.2. Unless the flaws are detectable and smaller than this critical dimension, it is recommended that any splice welds with visible cracks at the weld throat should be ground out as per priority 1 defects. Once the through thickness crack is removed, or 100mm of weld is removed, grinding should stop, and the flaws assessed as type 2b defects.

8.3.3 Bottom Flange Splice, defects at exposed root of ground/repaired welds (Type 2b)

This is the most critical defect type in the structure and the most difficult to detect and manage. The critical height of the residual defects is small. The length of the residual defect is difficult to determine with certainty due to proximity to the unfused land. The critical flaw depth versus length charts in Section 5.7.3 show that with increasing length the critical height plateaus at a value which is taken as

the recommended maximum height for the residual defect. These dimensions are summarised in Table 43.

It is essential that after grinding the cracked weld material, the exposed face with the residual defect is machined to a high surface finish. This not only removes potential crack initiation sites but increases the detection capability of MPI or PT.

If the measured height of the exposed flaw at the root exceeds the critical flaw height in Table 43 or the NDT system is not capable of detecting the required flaw size with confidence then the weld flaw is unacceptable and the risk of fracture must be reduced by:

- Reduce vehicle load (i.e. remove crane loads / centreline running)
- Reduce vehicle speed to reduce the stress level at the detail
- Other remedial solution to reduce the stress on the flawed detail.

Rewelding of the splice would return the weld to its original intended condition and reduce the stresses at the Type 2b defect which would be internal to the weld.

8.4 Risk of bridge collapse

As noted in section 7 of the report a fracture in the edge girder would be a more significant risk of structural collapse than a fracture in an internal girder. This is demonstrated by the number of elements and magnitude of the SAR values which are less than 1.

Improved redundancy could be provided by additional bolting of the cross girders to mobilise the reserve of bending strength which is available in the beam cross section.

It is noted that the assessment is carried out for ULS applied loads and ULS capacities however the loading on the bridge at failure would be reasonably expected to be at an SLS level. This application of ULS loads is justified since a brittle failure of a bridge girder would be a highly dynamic structural situation where DLA factors can be up to 1 (total DLA =2 rather than 1.4).

Direct measurement of the stresses in the bridge would allow for an improved load rating of the bridge through use of a measured DLA for regular traffic. It may also offer an early warning system in the event of a brittle fracture.

9 Further works

9.1 Existing MPI Investigation

The existing MPI inspection regime being undertaken by TMR should be completed to obtain a baseline assessment of the 72 splice locations on the bridge.

9.2 Other items

The flaws identified in this report are one element of the maintenance works identified for the bridge by TMR. Other issues include the following

- Long term durability, vibration control and corrosion of the Macalloy stressed bars.
- Risk of failure of the Macalloy stressed bars.
- Risk of rocker bearing instability at halving joints under longitudinal loading and / or thermal movements of the bridge. Refer to Figure 42 below for the detail.
- General corrosion of the bridge structure due to life expiry of the existing lead paint. The bridge requires renewal of the paint. Refer to Figure 42

These items need to be included in the development of the long-term management plan for the bridge.

Figure 42: Existing rocker bearings on bridge and corrosion on the steelwork